Green Chemistry

PAPER

View Article Online
View Journal | View Issue

Cite this: *Green Chem.*, 2023, **25**, 2409

Oxalic acid hydrogenation to glycolic acid: heterogeneous catalysts screening†

Eric Schuler,[a] Lars Grooten,[a] Mohanreddy Kasireddy,[b] Santosh More,[b] N. Raveendran Shiju,[a] Setrak K. Tanielyan,[b] Robert L. Augustine[b] and Gert-Jan M. Gruter *[a,c]

To meet our ambitions of a future circular economy and drastically reduce CO_2 emissions, we need to make use of CO_2 as a feedstock. Turning CO_2 into monomers to produce sustainable plastics is an attractive option for this purpose. It can be achieved by electrochemical reduction of CO_2 to formic acid derivatives, that can subsequently be converted into oxalic acid. Oxalic acid can be a monomer itself and it is a potential new platform chemical for material production, as useful monomers such as glycolic acid and ethylene glycol can be derived from it. Today the most common route from oxalic acid to glycolic acid requires multiple steps as it proceeds *via* oxalic acid di-esters as intermediates. In this work, we aim to avoid the extra reaction step of esterification. We explore the direct conversion of oxalic acid to glycolic acid in a two-step approach. In the first step, we define the ideal reaction conditions and test commercially available catalysts. We show that the reduction of oxalic acid can be performed at much lower temperatures and glycolic acid yields higher than those reported previously can be obtained. In the second step, we explore the design principles required for ideal catalysts which avoid the formation of acetic acid and ethylene glycol as side products. We show that ruthenium is the most active metal for the reaction and that carbon appears the most suitable support for these catalysts. By adding tin as a promotor, we could increase the selectivity and yield further whilst maintaining high activity of the resulting catalyst. This research lays the foundation for the efficient direct reduction of oxalic acid to glycolic acid and defines the design parameters for even better catalysts and the ideal process and conditions.

Received 28th June 2022,
Accepted 27th February 2023

DOI: 10.1039/d2gc02411j

rsc.li/greenchem

Introduction

As we strive to reduce atmospheric CO_2 levels, we need to find sustainable alternatives to fossil feedstocks. Today, the chemical industry is a major greenhouse gas emitter that relies on fossil-based feedstocks.[1] However, unlike many other sectors, the chemical industry can use CO_2 as a feedstock and turn from a non-circular CO_2 emitting industry to a circular industry providing a net carbon sink.[2–7] In fact, the only non-fossil alternative carbon sources to produce carbon-based materials or fuels are biomass and CO_2.[8,9] CO_2 is an economically interesting feedstock as it has low or even negative costs and is highly abundant.[2,8,10,11] Yet many routes leading to valuable products from CO_2 require improvements before becoming commercially viable.[12,13] One of those routes (Fig. 1) is aiming at polymers from CO_2 with oxalic acid at the end as a platform chemical for monomers and other chemicals.[14,15]

Oxalic acid, the simplest of the dicarboxylic acids, is one of the oldest known acids which was discovered by Scheele in 1734.[16] Oxalic acid can be used as a platform chemical to produce well-known compounds such as mono ethylene glycol, glyoxylic acid, glyoxal, glycolaldehyde and glycolic acid.[17] All five C2 compounds derived from oxalic acid are of increasing interest for the manufacture of high-performance polymers. Ideally, monomers for sustainable polymers should be derived by linking the consumption of CO_2 with the production of circular, potential long-term carbon storage in materials.

In this work, we focus on the fourth step of the OCEAN process (Fig. 1), the reduction of oxalic acid to glycolic acid. We aim to identify key parameters for catalyst design and reaction conditions. Our primary indicator at this stage is catalyst performance defined by its activity, selectivity and stability. The most suitable options are developed further and we investigate the reasoning behind their superior performance in greater detail in a follow-up study. As oxalic acid from other

[a]*Van 't Hoff Institute for Molecular Sciences, University of Amsterdam, Science Park 904, 1090 GD Amsterdam, The Netherlands. E-mail: g.j.m.gruter@uva.nl*
[b]*Department of Chemistry and Biochemistry, Green Chemistry Academy, Seton Hall University, South Orange, NJ, USA*
[c]*Avantium Chemicals BV, Zekeringstraat 29, 1014 BV Amsterdam, The Netherlands*

† Electronic supplementary information (ESI) available. See DOI: https://doi.org/10.1039/d2gc02411j

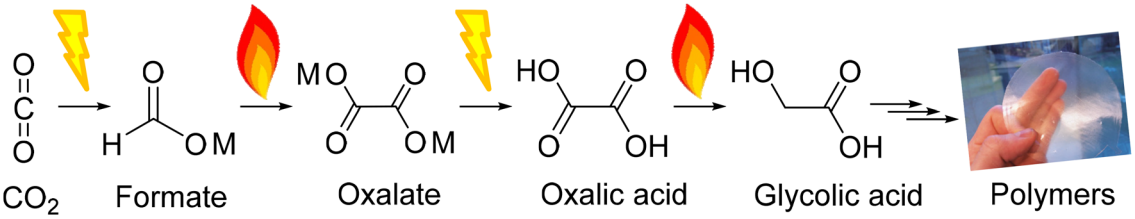

Fig. 1 "OCEAN" process for CO_2 utilization *via* (i) electrochemical reduction to formate, (ii) thermal formate coupling to oxalate, (iii) electrochemical oxalate acidification, (iv) thermocatalytic reduction of oxalic acid to glycolic acid, and (v) polymer production from oxalic acid and its derivatives.

renewable sources is available (CO_2, CO, formate, ethylene glycol, ethylene, and sugars) this work is also applicable to these processes.[17] Glycolic acid is an alpha-hydroxy acid that occurs naturally in many fruits such as grapes, pineapple, sugarcane, cantaloupe, and sugar beets. Moreover, glycolic acid is an interesting compound in the development of new polymers for which a detailed account from our group was published recently by Murcia *et al.*[18]

The glycolic acid market volume in 2020 was 310 M$ and is projected to reach 530 M$ by 2027.[19] Based on our work on glycolic acid production and applications,[18] we expect that with much lower glycolic acid prices the PLGA polyester volume potential can be much larger than these projections. Several commercial routes towards glycolic acid exist today. They include the hydrolysis of methyl glycolate or glyconitrile, both produced from methanol; the hydrolysis of chloroacetic acid obtained from acetic acid; and the carbonylation of formaldehyde which today is the dominant industrial production method.[20–26] All these routes are fed by fossil feedstocks today. In the future fossil feedstocks need to be replaced by sustainable carbon and energy sources. Zhou *et al.*, suggested to produce glycolic acid from ethylene glycol using biomass as a source for carbon and energy.[27] Their technoeconomic analysis shows that this process is favourable over existing fossil processes. However, with growing land use pressure in the future – we believe that the only truly sustainable carbon source of the future is CO_2.[28,29] Hence, all feedstocks for sustainable glycolic acid should be obtained from CO_2 and water. This allows to perform a species comparison based on the complexity of the different routes towards glycolic acid. The overall reaction from CO_2 and water to glycolic acid is independent of the pathway and requires two CO_2 molecules and two water molecules, leading to an overall standard enthalpy of reaction $\Delta_{rxn}H$ = 775.7 kJ mol^{-1}. However, each route requires a different number of steps (Table 1, Fig. S17†). The production of glycolic acid from CO_2 *via* direct electrochemical oxalate formation followed by acidification to oxalic acid and hydrogenation of oxalic acid to glycolic acid requires five steps ((i) $2CO_2$ + Zn to $Zn(C_2O_4)$ (oxalate); (ii) $Zn(C_2O_4)$ to $C_2H_2O_4$ (oxalic acid) and (iii) Zn^{2+} to Zn; (iv) $2H_2O$ to $2H_2$ and O_2 and (v) $C_2H_2O_4 + 2H_2$ to $C_2H_4O_3$ (glycolic acid) + H_2O) and thus the least steps of all pathways.

In a simplified approach we estimate the cost price for the production of glycolic acid assuming optimal heat integration using 200$/ton processing fee for each step, CO_2 and water at zero cost, an electricity price of 50$/MWh, a fully optimized mature process with 50% power efficiency, and a default optimal yield of 98% for each step independent of the pathway.[30] The estimated cost price for each route with sustainable feedstocks is shown in Table 1. The reduction of oxalic acid proposed here has the lowest overall cost-price ($1316) and is thus a valid option to produce sustainable glycolic acid in the future.

Table 1 Comparison of reaction steps and resulting cost price for sustainable production of glycolic acid using CO_2, water and renewable energy as feedstock. For the estimation of the cost price, we assume a 50% power efficiency, 98% yield per step, 200$/step processing fee and an electricity price of 50$/MWh

Reaction	Steps	Estimated cost price ($/ton)
Carbonylation of formaldehyde	7	1729
Glyconitrile route	7	1729
Chloro acetic acid route	10	2350
Methyl Glycolate route	9	2143
Hydrogenation of Oxalic acid	5	1316

A short history of the oxalic acid hydrogenation

Carboxylic acid reduction catalysed by ruthenium-based catalysts is known since the 1950s and ever since many applications were reported in the literature.[31–34] However, before the start of this work, only a general publication for the reduction of organic acids to alcohols by Carnahan *et al.* covered the catalytic reduction of oxalic acid using a ruthenium catalyst. They reduced oxalic acid using ruthenium dioxide as a catalyst and produced ethylene glycol at temperatures between 94–150 °C.[35] Notably, they used very high hydrogen pressures of 630–900 atmospheres and long reaction times of 10 hours. Although they didn't produce glycolic acid from oxalic acid, they used glycolic acid as a reactant. They found that glycolic acid could be effectively reduced to ethylene glycol at temperatures above 110 °C. Both ruthenium oxide and commercially available ruthenium on carbon were suitable catalysts but platinum and palladium were ineffective as catalysts. Overall, they noted that higher yields could be achieved if the acids were first converted to esters and then reduced to the desired products. Our work started as a collaboration between Seton Hall University and Liquid Light Inc.

initially. After the acquisition of Liquid Light by Avantium the University of Amsterdam got involved and developed the process further. Until the start of our work, only the catalytic reduction of oxalic acid esters was an active field of research.[36–41] We used the findings of Carnahan *et al.*, as a starting point for our work. Yet, so have others and both Lange *et al.*, and Santos *et al.*, have since reported further details on the reduction of oxalic acid to glycolic acid and ethylene glycol using heterogeneous catalysis.[42,43]

Lange *et al.*, presented a process to produce glycolic acid from oxalic acid. Their process made use of a hydrogenation metal catalyst and they used 4 wt% ruthenium supported on TiO_2 as a catalyst in their examples.[42] The lowest temperature in their examples is 100 °C at which they achieved their highest glycolic acid yield of 76% at 80% conversion after 4 hours in batch. As this reaction is already quite slow at 100 °C, lower temperatures were not investigated. At higher temperatures of 120 °C and 135 °C, the glycolic acid yield dropped to 6% and ethylene glycol was produced primarily. They recommend the use of hydrogen pressures below 150 bar and a starting concentration of oxalic acid between 5 and 25 wt%. Although they define the ideal metal loading of the catalyst as 2–20 wt%, they do not explain the role of the metal in the catalyst, effects of catalyst preparation methods or the role of the support further and only show examples with ruthenium-based catalysts. Interestingly, they found that contrary to the reports of Carnahan *et al.*, the presence of water did not cause the decomposition of oxalic acid.[35]

The most recent report from Santos *et al.*, discusses the mechanism of oxalic acid reduction using ruthenium supported on carbon as catalysts. They studied the reaction in a slurry reactor with self-made catalysts and fitted a kinetic model to their results to investigate the mechanism. They achieved a glycolic acid selectivity of 70% at 120 °C where they produced 70.6% glycolic acid, 15% acetic acid and 15% ethylene glycol at an oxalic acid conversion of 90%. When increasing the temperature to 150 °C stepwise, they observed a shift towards the production of volatile compounds.

Santos *et al.*, also suggested a Langmuir–Hinshelwood mechanism as shown in Fig. 2, with distinct sites for oxalic acid and hydrogen adsorption. First, oxalic acid is adsorbed by an interaction of the C=O bond of the carboxylic acid groups with a ruthenium site (θ_A) of the catalyst. Molecular hydrogen adsorbs on an acid-activated carbon (θ_B) site. In a second step, a reaction occurs by hydrogen transfer to the adsorbed oxalic acid. This results in a de-hydroxylation step that yields glyoxylic acid. After, the hydrogenation of oxalic acid to glyoxylic acid, the glyoxylic acid is reduced to glycolic acid and desorbs from the surface. As glyoxylic acid can't desorb from the surface, it cannot be observed in this system. The reaction of oxalic acid to glycolic acid follows the same mechanism as the reduction of glycolic acid to ethylene glycol. Effectively, the formation of ethylene glycol requires the reduction of both acid groups. The formation of acetic acid however proceeds *via* the hydrogenolysis of the H_2C–O bond. Interestingly, the reduction of the second acid group to form ethylene glycol

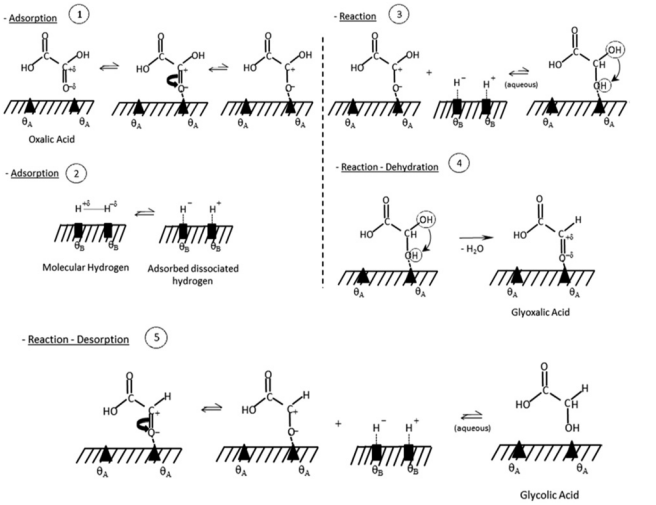

Fig. 2 Reaction mechanism for oxalic acid hydrogenation reproduced with permission from Santos *et al.*[43]

from glycolic acid has a lower energy barrier of 16 kJ mol^{-1} compared to 17.8 kJ mol^{-1} for the reduction of oxalic acid to glycolic acid. However, according to Santos *et al.*, oxalic acid adsorbs much easier on the catalyst as it has two acid groups and therefore the oxalic acid to glycolic acid reduction is dominant. The role of the much lower pK_A of oxalic acid (1.27) which is the lowest of all carboxylic acids, was not considered. This means that 5% of oxalic acid are present as anion compared to 0.2 ‰ of glycolic acid (pKa 3.83) which should favour oxalic acid adsorption. The formation of acetic acid has a higher activation barrier of 23 kJ mol^{-1}. Overall, this results in the reaction scheme illustrated in Fig. 3.

Ruthenium based catalysts

Ruthenium is widely used as a hydrogenation catalyst.[35,44–46] As carboxylic acid reduction depends on the adsorption of the acid group on the catalyst surface, we also drew inspiration from work on other substrates such as the reduction of lactic acid, adipic acid but also fatty esters or aldehyde reductions. Takeda *et al.*, investigated the hydrogenation of lactic acid to 1,2-propanediol using modified ruthenium on a carbon catalyst containing a small percentage of molybdenum.[47–49] The addition of molybdenum increased the turnover frequency (TOF) compared to the mono-metallic ruthenium catalyst as molecular hydrogen can dissociate easier at the intersection of the ruthenium metal and molybdenum oxide species. The addition of tin to ruthenium-based catalysts is used in many hydrogenation reactions.[46,50–55]

Active metals for hydrogenation reactions

Although most popular, ruthenium is not the only metal reported for the reduction of carboxylic acids or CO_2. Kong *et al.*, investigated the hydrogenation of dimethyl oxalate (DMO) to ethylene glycol by using a CuMg/ZnO catalyst.[56] All of the DMO was converted in their reaction, with about 95%

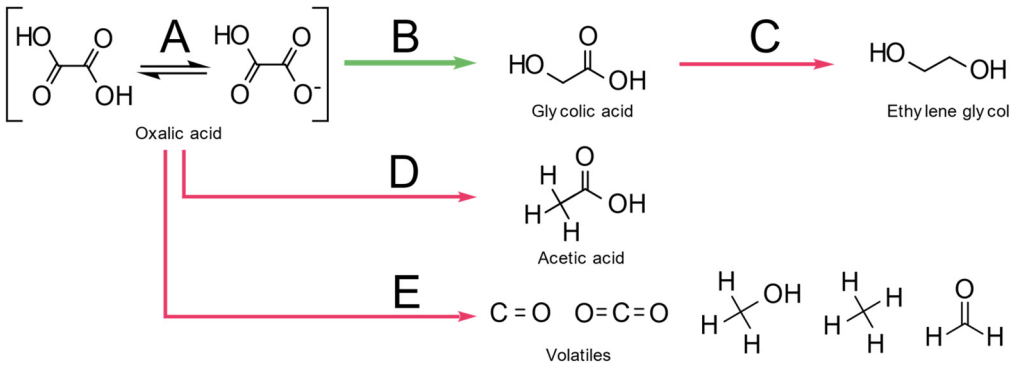

Fig. 3 Reaction pathways in the hydrogenation of oxalic acid. (A) Deprotonation of oxalic acid in water (pK_a = 1.27). (B) Desired route to Glycolic acid (17.8 kJ mol^{-1}). (C) Overreduction to ethylene glycol (16 kJ mol^{-1}). (D) Formation of Acetic acid (23 kJ mol^{-1}). (E) Decomposition to volatile compounds dominant at temperatures above 120 °C.

selectivity for ethylene glycol. The catalyst proved stable for 300 hours. Pouilloux *et al.*, replaced a ruthenium-tin catalyst with a cobalt-tin catalyst for the hydrogenation of methyl oleate to oleyl alcohol and reported similar selectivity but lower conversion.[57,58] Wang *et al.*, report the NiFe/C catalysed selective hydrogenation of stearic acid to stearic alcohol.[59] They examined different metal ratios and observed the best performance (98% selectivity and 100% conversion) for a metal ratio of $Ni_{1.8}Fe_{1.5}$. Ni_3Fe particles on the surface of the catalyst were responsible for the activity. Tayao *et al.*, examined many different metals (Re, Pt, Ir, Ru, Rh, Pd, Ag, Cu, Ni, and Co) supported on titania catalysts for the hydrogenation of 3-phenyl propionic acid and reported the highest conversion and selectivity with a rhenium catalyst.[60] They then used these 2 wt% Re/TiO2 catalysts and reached alcohol yields of 90% in the hydrogenation of 14 different carboxylic acids. High-surface area indium oxide nanoparticles were used successfully in the hydrogenation of CO_2 to methanol by Frei *et al.*, and can be produced in an easy synthesis.[61]

Our goal is to develop a process for the reduction of oxalic acid to glycolic acid and avoid the over reduction to ethylene glycol and the formation of volatiles or acetic acid. We use a high-throughput screening approach with a strong emphasize on catalyst performance testing to identify key parameters for catalyst design and reaction conditions. We would like to emphasize, that this work is intended to inform on the influence of each parameter as independently as possible and should not be read as a consecutive approach in which we stepwise exclude parameters. This work is the culmination of two independent studies performed at Seton-Hall University and the University of Amsterdam over the span of 8 years. We decided to combine this work to allow the reader a comprehensive overview of the key parameters for this reaction. We establish suitable conditions for the reaction using a commercially available ruthenium catalyst known to perform well for carboxylic acid reduction. The variables include reaction temperature and pressure, reaction time and stirring rate, pre-reduction of the catalyst and catalyst loading, reactant concentration and reactor materials. We explore the suitability of hydrogenation catalysts introduced above and develop new catalysts for which we vary the support material and active metal, the metal loading and secondary metal, metal precursors and catalyst-preparation methods.

Experimental

We performed all reactions at the University of Amsterdam (UvA), Avantium or Seton Hall University (SHU). The batch reactors used at Avantium allow for performing reactions and testing many variables in parallel.[62] In this setup sampling rates are limited and only liquid samples can be analysed. At SHU we used a single batch reactor which allows for high sampling rates and analysis of liquid and gas phase and monitoring of gas consumption during the reaction, yet only one catalyst could be tested at a time. In a first step at SHU we optimized reaction conditions including reaction temperature (75–150 °C), hydrogen pressure (0–150 bar), reaction time (1–24 h), oxalic acid concentration (5–20 wt%) and investigated the role of reactor materials. At the UvA we used the ideal reaction combinations determined at SHU to test newly developed catalysts.

All chemicals, metal precursors and support materials were reagent grade and obtained from Sigma-Aldrich. The catalysts used during this work included commercial catalysts, reproductions of catalysts presented in literature and new catalysts developed in-house. We obtained commercial catalysts shown in Table S3† from Johnson Matthey, Alfa Aesar and Sigma Aldrich. For the preparation of catalysts presented in the literature, we followed their synthesis protocols (for details see ESI 3.1–3.5†) there. During the development of new catalysts, we used incipient wetness impregnation) at the SHU (for details see ESI 3.6†) and wet impregnation at UvA (for details see ESI 3.7†). After impregnation, all catalysts were calcined and reduced under a 7% hydrogen atmosphere at 350 °C for 3 hours in a tubular furnace. Before use, the catalysts were analysed using nitrogen adsorption analysis at 70K in a BELSORP-Max II (BET) pre-treated at 180 °C for 6 hours in

vacuum and X-ray diffraction (XRD) measurements using a Rigaku Miniflex at an angle (2θ) of 3 to 90 degrees at a rate of 1° min^{-1} and a step size of 0.05°. After the reaction, a qualitative and quantitative analysis of liquid products was performed by liquid chromatography measurements. At Seton Hall University the samples were prepared by diluting the samples in the mobile phase and adding internal standards. A Shimadzu HPLC instrument with refractive index detector (RID) was used to measure the concentration of oxalic acid, glycolic acid, glyoxylic acid, acetic acid, and ethylene glycol. The exact conditions are listed in Table S6†. At the University of Amsterdam the samples were prepared by diluting the samples in demineralized water to a theoretical stock solutions concentration of 0.67 mg stock mL^{-1}. High Performance Liquid Chromatography (HPLC) was used to determine oxalic acid, glycolic acid, glyoxylic acid, acetic acid, and ethylene glycol concentration on an Agilent 1260 Infinity II HPLC system equipped with an autosampler, heated column compartment, diode-array detector (DAD) and RID. The column was an Aminex HPX-87H (300 × 7.8 mm; dp 9 μm). All conditions are listed in Table S7.†

The qualitative and quantitative analysis of gaseous reaction products was performed using a HP 5890 gas chromatograph with FID detector (for details see ESI section 5†).

Results and discussion

In our previous work, we discuss the formate coupling reaction to oxalate and oxalic acid which is an interesting feedstock for new polymers.[17,18,63,64] Next to oxalic acid as monomer itself (which thermal instability can be overcome by using appropriate ester derivatives) it can also be the starting material for other monomers.[65–67] One of those is glycolic acid for which one of the acid groups is reduced to an alcohol. Effectively this can be done by first converting the oxalic acid into an ester and then reducing the ester to glycolic acid. In this work, however, we desire to evaluate the boundary conditions under which oxalic acid can be directly reduced to glycolic acid. We identified potential reaction products, determined a range of reaction conditions and tested interesting catalyst concepts, newly developed and commercially available catalyst for the reaction.

Products, temperature, and reaction time

First we aim to explore and optimize the reaction conditions starting with reaction temperature and time. In principle, oxalic acid can be converted in two ways: Either we reduce the acid groups to aldehydes (such as glyoxylic acid) and alcohols (glycolic acid or ethylene glycol) or we decompose it to single carbon compounds such as formic acid and CO_2. These products can be divided into volatile compounds found in the gas phase after the reaction, and dissolved solids or liquids found in the aqueous phase. We started by first assessing the thermal stability of oxalic acid in a hydrogen atmosphere in the absence of a catalyst and started in a 140–170 °C temperature range (details ESI 4.8†). We show that oxalic acid is highly unstable and decomposed completely at 150 °C and 170 °C (Table S1 and Fig. S3†). This decomposition occurs within the first two hours of reaction and the main reaction products are formic acid (found in the aqueous and gaseous phase) and CO_2 (gas phase). When the reaction temperature was lowered to 140 °C, the rate of decomposition was reduced significantly. The decomposition after two and four hours were 20.9% and 29.4% respectively, and near-complete decomposition was observed after 21 h. Consequently, efficient hydrogenation of oxalic acid can only be accomplished at reaction temperatures below 140 °C.

The analysis of both the aqueous and the gas phase shows that the main thermal decomposition product is formic acid and CO_2. This is in line with the suggestion for using reaction temperatures lower than 140 °C as stated by Lange *et al.*[42] However, we found a more diverse range of decomposition products compared to Santos *et al.*[43] We repeated the experiment at 170 °C in the presence of hydrogen (100 bars) and a catalyst (5 wt% Ru/C). The oxalic acid was completely consumed in the first two hours and glycolic acid and formic acid were formed at 18% and 20% selectivity (Table S2, Fig. S4†). After this initial 2-hour period, the formic acid decomposed further while the glycolic acid was converted to ethylene glycol at a 5–6 times lower rate compared to the oxalic acid to glycolic acid hydrogenation. The analysis of the gas phase showed the presence of CO_2, CO, Methanol, Formaldehyde, Methane and C_2–C_6 hydrocarbons.

As we are primarily interested in the production of glycolic acid, we reduced the temperature to a range of 75–130 °C (details ESI 4.9†). We took samples every hour of the reaction for a total span of 5 hours as shown in Fig. 4. The reactions at 120 °C and 130 °C were continued for another 15 hours as shown in Fig. 7 and S3.† With increasing temperature, the conversion increased. At 130 °C almost all the oxalic acid (92%) was converted after 1 hour, whilst at 75 °C, 30% of the oxalic acid was still left after five hours of reaction. The glycolic acid yield continually increased with time at 75, 80 and 85 °C. The highest glycolic acid yield of 76% equalling the best result of Lange *et al.*, was already achieved at 85 °C after 5 hours of reaction whilst Lange *et al.*, required 100 °C and 4 hours (Fig. 4B).[42] At higher temperatures, the glycolic acid yield decreased over time, especially at 130 °C. This was caused by the over-reduction of glycolic acid to ethylene glycol with increasing temperatures (Fig. 4C). In Fig. 4A and B, we can see that reduction of oxalic acid is preferred over the reduction of glycolic acid to ethylene glycol. At 100 °C (red) and 120 °C (dark blue), the glycolic acid yield increased until the oxalic acid was fully converted. However, the formation of ethylene glycol from glycolic acid already started to increase when 70% of oxalic acid was converted. After full oxalic acid conversion, the ethylene glycol yield rises strongly and the glycolic acid yield declines. With lower amounts of oxalic acid present, more and more active sites become available for the adsorption of glycolic acid and its subsequent reduction to ethylene glycol. Overall, higher temperatures allow reaching high glycolic acid yield quicker and the over reduction to ethylene glycol can be controlled by reducing the reaction time. However,

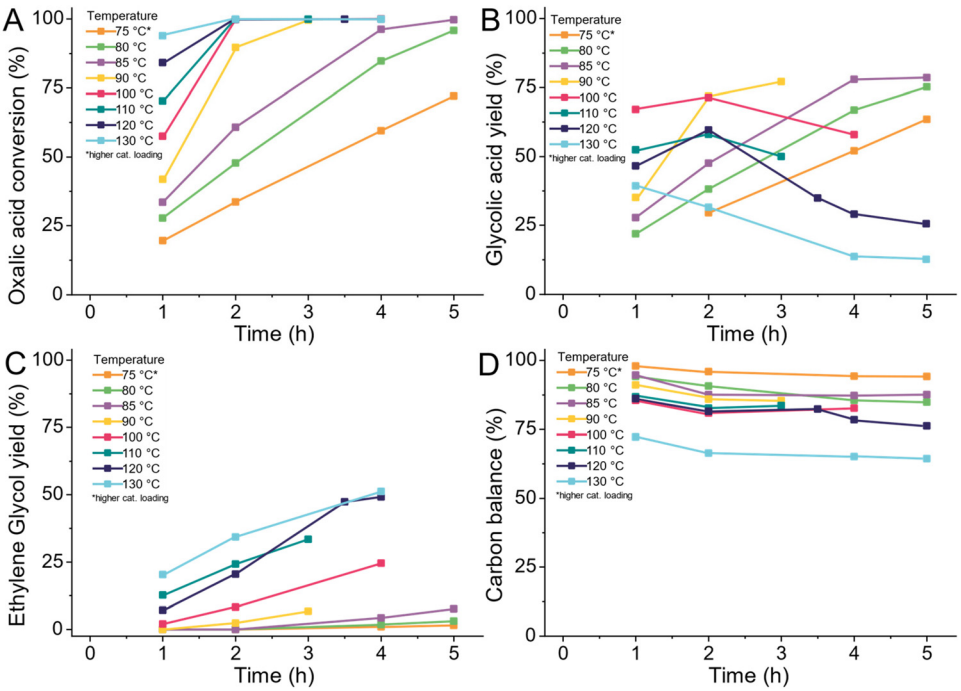

Fig. 4 Influence of reaction temperature on the reduction of 5% oxalic acid in aqueous feed on (A) oxalic acid conversion, (B) glycolic acid yield, (C) ethylene glycol yield, and (D) carbon balance. All reactions were performed using a 100 mL all Hastelloy batch reactor filled with 0.275 g (0.45 g for 75 °C) of 5 wt% Ru/C (Johnson Matthey, type 5R600) catalyst, reduced at 250 °C no pre-reduction in the reactor; substrate = 41.5 g of 5 wt% aqueous oxalic acid; stir rate = 400 rpm; pressure = 100 bar H2; temperature = 75 °C – 130 °C.

lower reaction temperatures are still preferable as the acetic acid production and formation of volatile compounds increase with higher temperatures. The formation of volatile compounds expresses itself in a decrease of the overall carbon balance shown in Fig. 4D. The trend again shows a decrease in the carbon balance with temperature. Above 120 °C, the formation of volatile compounds increased strongly. Interestingly, no volatiles formed from ethylene glycol or glycolic acid as the carbon balance stayed stable at prolonged reaction times as shown in Fig. S5D.† Due to the high production of volatiles and acetic acid at higher temperatures, we narrowed the temperature range to 75–105 °C. In the second set of experiments, we increased the concentration of oxalic acid from 5 wt% to 10 wt% and pre-reduced the catalyst in the reactor to increase its activity. As Fig. S6A† shows, the conversion increases with temperature and ethylene glycol production increases once oxalic acid reaches full conversion. Glycolic acid was reduced to ethylene glycol even at 75 °C with longer reaction times. The overall carbon balance was again higher at lower temperatures (Fig. S6D†). The selectivity towards acetic acid was independently high with an average of selectivity of 9% at 75, 85 and 95 °C. At 105 °C, the production of acetic acid increased to 15%, which is in agreement with the higher activation energy required for this reaction according to Santos *et al.*[43]

Overall, various products were formed by a combination of pathways as illustrated in Fig. 5. At temperatures above 120 °C oxalic acid decomposes mainly to formic acid and CO_2 following pathway a. The desired hydrogenation pathway A leads to the glycolic acid as described by Santos *et al.*[43] Glycolic acid can also be further hydrogenated towards ethylene glycol in pathway B. At higher reaction temperatures, the decomposition of oxalic acid, glyoxylic acid, and glyoxal leads to the formation of CO_2, CO and formaldehyde following pathway b. Formaldehyde is the main precursor to higher hydrocarbons (pathway c) and methanol (pathway d). Methanol can be further reduced to methane *via* pathway e. Acetic acid is formed in a parallel reaction as has been proposed by Santos *et al.*[43] The formation of glycolic and acetic acid probably takes place through a common intermediate which either is hydrogenated to Glycolic acid (path A) or trough hydrogenolysis generates Acetic acid (path C). Based on the results from the thermal decomposition and catalytic hydrogenation reactions, we propose, that the overall oxalic acid conversion in the presence of a 5 wt% Ru/C catalyst takes place through a series of reactions *via* pathway a–e (thermal decomposition) and pathways A and B (catalytic hydrogenation), and pathway C (acetic acid formation). The overall rate ratio between the pathways depends on the reaction temperature, the catalyst, the hydrogen pressure, and the solvent. For efficient hydrogenation of oxalic acid to take place, the reaction temperature should probably be below 100 °C to keep the rate of thermal decomposition sufficiently lower than the hydrogenation rate along with pathway A. Given the low solubility of oxalic acid compared to glycolic acid, the separation of reactant and product can be achieved by crystallization. The separation of ethylene glycol and acetic acid from glycolic acid however is more chal-

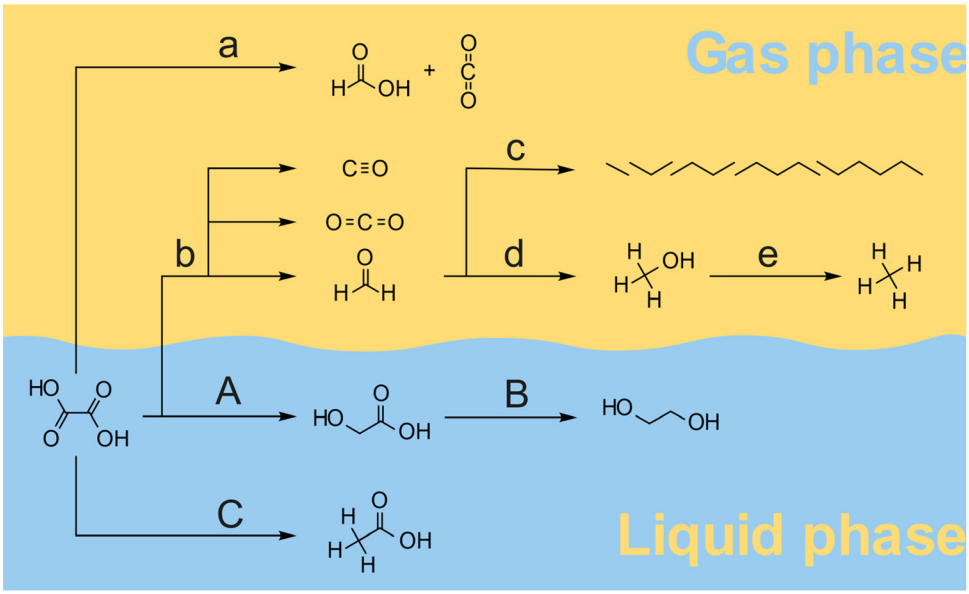

Fig. 5 Reaction pathways for the decomposition and hydrogenation of oxalic acid leading to products observed either in the gas phase or liquid phase after the reaction. (a) At high temperatures above 140 °C, oxalic acid predominantly decomposes to formic acid and CO_2 (formic acid was also found in the liquid phase); (b) the glyoxal intermediate can decompose to formaldehyde, CO, and CO_2; Formaldehyde can decompose further towards (c) alkanes (ethane to hexane were detected in gas-phase) or (d) methanol which can be reduced further towards (e) methane (both methanol and methane were detected in the gas phase). (A) At temperatures below 140 °C the formation of the desired glycolic acid is favoured over the formation of volatiles. (B) Glycolic acid can be reduced further towards ethylene glycol. (C) Acetic acid is produced in a competing reaction that occurs in parallel to the glycolic acid formation but at a lower rate. All compounds were detected in the aqueous phase during this work.

lenging as all dissolve well in water. Hence, it is highly desirable to avoid the formation of these side-products not only to improve the overall yield but also to avoid a costly downstream separation process.

We decided to continue our work using a reaction temperature of 75 °C as this avoids the formation of volatiles. We did not reduce the temperature further at this stage as the required reaction times were already long and we decided to explore lower temperatures at a later stage, after developing a more active catalyst which we will be presenting in an upcoming publication. Compared to Lange *et al.*, and Santos *et al.*, we could show that using reaction temperatures below 100 °C is beneficial to prevent the formation of acetic acid and especially volatiles.[42,43] Even without further optimizing the reaction conditions, we could achieve higher yields of glycolic acid compared to both previous publications. Lower temperatures require longer reaction times which we attempt to counteract with increased catalyst loadings and higher hydrogen availability at higher hydrogen pressures.

Hydrogen pressure

To reduce oxalic acid to glycolic acid and ethylene glycol the co-reactant hydrogen is supplied as gas. Hydrogen must dissolve in the reactant solution to reach the active sites of the catalyst. Consequently, the pressure of hydrogen dictates the availability of hydrogen for the reaction as its solubility increases with pressure. We tested the effect of three hydrogen pressures of 50, 100 and 135 bar at the reaction temperature. As a negative control, we pressurized the reactor with 40 bar of inert Argon (details ESI 4.10†).

In the absence of hydrogen, at 75 °C, in the presence of 5 wt% Ru/C catalyst, oxalic acid is neither reduced nor decomposed to volatiles (Fig. 6B–D). With increasing hydrogen pressure, the conversion of oxalic acid increased as Fig. 6A shows. When increasing the pressure from 50 bar to 100 bar, the oxalic acid conversion increased 30% to 92% (after 7 hours reaction). Increasing the pressure to 135 bar only increased the conversion with 8% from 68% to 76% (after 4 h of reaction). The hydrogen pressure did not influence the selectivity or increase the formation of volatiles as the carbon balance stayed constant for all pressures as shown in Fig. 6D. Consequently, a higher hydrogen pressure is beneficial for the reduction of oxalic acid to glycolic acid. If all other parameters are kept equal, higher hydrogen pressures increase the reaction rate and allow for shorter reaction times. For the catalyst development, we continued using a pressure of 100 bar.

Catalyst loading

As the reaction is catalysed by an active metal site, increasing the number of metal sites in the reactor should increase the overall reaction rate. The number of active sites can be changed by increasing either the amount of metal on the catalyst itself, by changing the amount of catalyst in the reactor, or by increasing the available active surface with a smaller catalyst particle size.

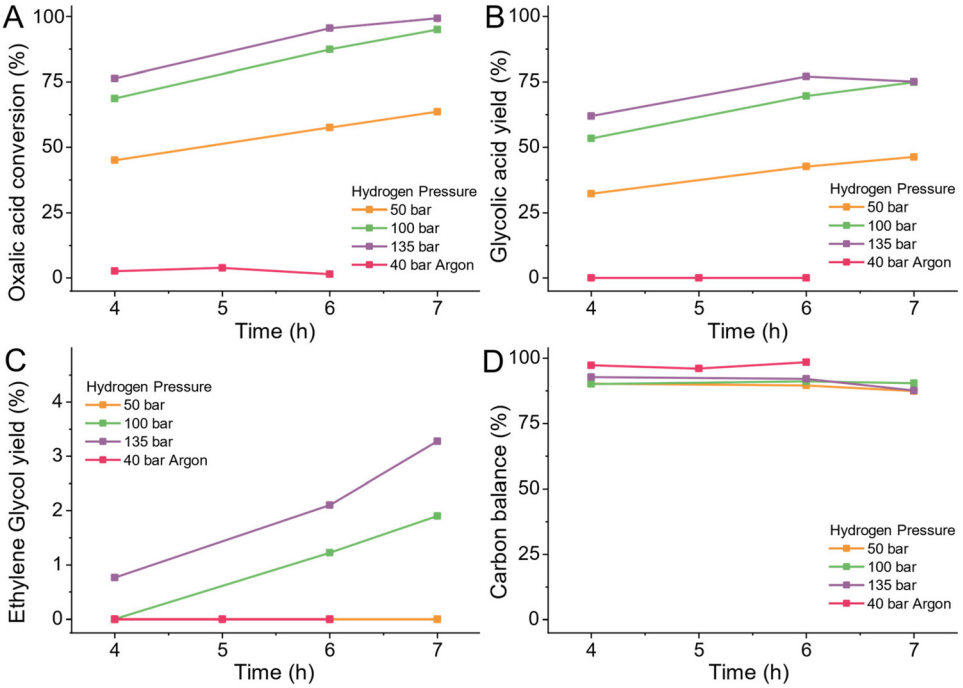

Fig. 6 Influence of hydrogen pressure on the reduction of 25% oxalic acid in aqueous feed on (A) oxalic acid conversion, (B) glycolic acid yield, (C) ethylene glycol yield, and (D) carbon balance. All reactions were performed using a 100 mL all Hastelloy reactor filled with 1.125 g of 5 wt% Ru/C (Johnson Matthey, type 5R600) reduced at 300 °C for 3 h then pre-reduced in the reactor at 100 °C; substrate = 41.5 g of 25 wt% aqueous oxalic acid; stir rate = 400 rpm; pressure = 50–135 bar H2 or 40 bar Argon; temperature = 75 °C.

We tested three metal loadings and three different amounts of catalyst (details ESI 4.11†). In both cases, we observed a linear increase in conversion with the increase in active metal (Fig. 7A). The selectivity for glycolic acid and ethylene glycol was not affected. The formation of acetic acid was independent of the metal loading and fluctuated between 7.9–11.5%. The introduction of higher metal loadings increased the formation of volatiles especially at long reaction times (Fig. S7D†).

Reactant concentration

Like the concentration of active sites on the catalyst, we can also change the initial substrate concentration therefore the total amount of reactant per unit available active sites. In general, using a highly concentrated feed solutions, particularly for batch reactors is highly desirable as it reduces the downtime required for filling and emptying the reactor. In the case of oxalic acid, changing the reactant concentration is limited by the low solubility of oxalic acid in water especially at lower temperatures (<5 wt% at room temperature).

We tested three different concentrations of 10, 15 and 20 wt% oxalic acid at 75 °C (details ESI 4.12) and observed a linear increase in the required reaction time to reach equal conversions (Fig. 8A and S8A†). The selectivity towards glycolic acid, ethylene glycol and acetic acid was not affected by the oxalic acid concentration (Fig. 8B and C). Higher oxalic acid concentrations reduced the volatiles production slightly. In a commercial application, higher concentrations of oxalic acid can be realized by pre-solvation of oxalic acid in water in a heated tank which feeds the heated reactant directly to the reactor. This should allow for an overall reduction of volatiles production and higher utilization of the reactors.

Ex situ and *in situ* catalyst reduction

To reach high activity, it is not only important to supply the right amount of catalyst but also to supply it in the activated – usually the reduced - form. The catalyst, therefore, must be reduced before use in the presence of hydrogen and the reduction temperature depends on the active metals. We explored the ideal reduction temperature in and *in situ* pre-reduction conditions in the reactor. For the reduction of the commercial 5 wt% Ru/C catalysts, we used reduction temperatures from 300 °C to 430 °C (details ESI 4.13.† A reduction at 350 °C led to the most active catalyst (Fig. S9A†). The selectivity towards glycolic acid, ethylene glycol and acetic acid was not affected by the reduction temperature. We compared the *in situ* pre-hydrogenation temperature at 100 °C and 200 °C for 1 hour and observed no difference in their activity. The generally beneficial effect of pre-hydrogenation of the catalyst in the reactor prior reaction can be observed when comparing the conversion activity in Fig. S9A† (no *in situ* pre-reduction) and Fig. S6A† (with *in situ* pre-reduction; note that twice the amount of oxalic acid was introduced for pre-hydrogenated catalysts). The insertion of this *in situ* pre-hydrogenation step of the catalyst allows the reaction to be carried out at much lower

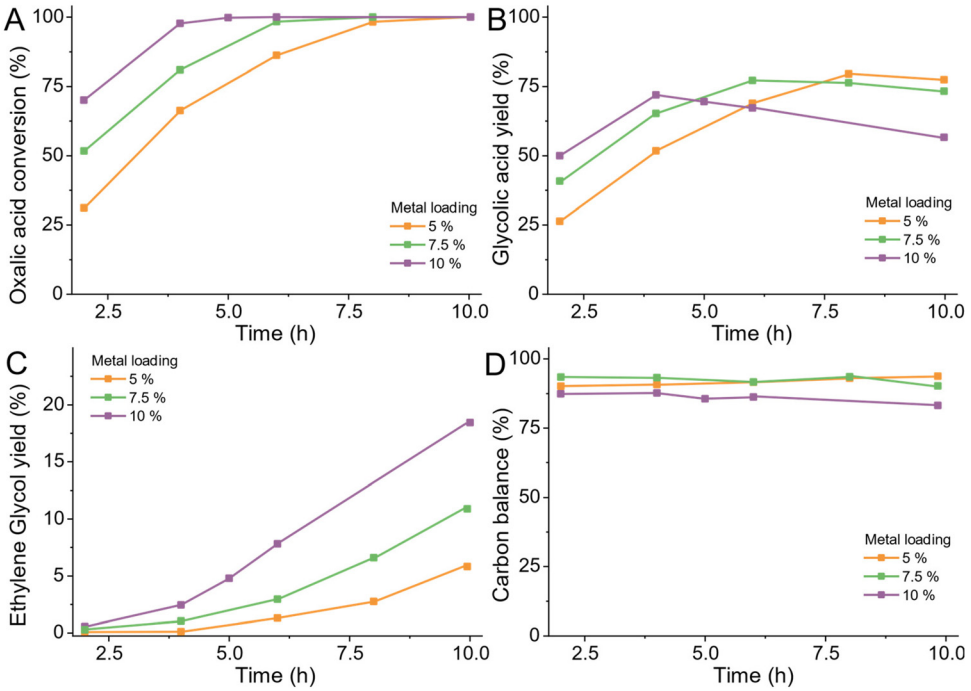

Fig. 7 Influence of metal loading on the reduction of 25 wt% oxalic acid in aqueous feed on (A) oxalic acid conversion, (B) glycolic acid yield, (C) ethylene glycol yield, and (D) carbon balance. All reactions were performed using a 100 mL all Hastelloy batch reactor filled with 1.125 g of 5 wt% Ru/C (Johnson Matthey, type 5R600), 7.5 wt% Ru/C (Johnson Matthey, type D102023–7.5), 10 wt% Ru/C (Johnson Matthey, type D101023–10), reduced at 300 °C then pre-reduced in the reactor at 100 °C; substrate = 41.5 g of 25 wt% aqueous oxalic acid; stir rate = 400 rpm; pressure = 100 bar H2; temperature = 75 °C.

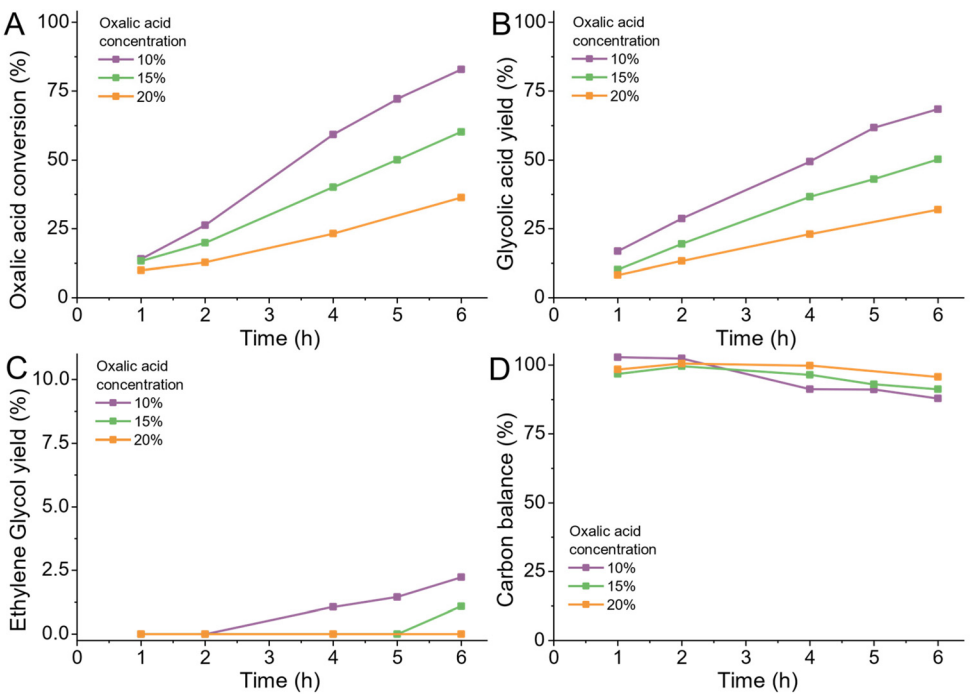

Fig. 8 Influence of oxalic acid concentration in aqueous feed on (A) oxalic acid conversion, (B) glycolic acid yield, (C) ethylene Glycol yield, and (D) carbon balance. All reactions were performed using a 100 mL all Hastelloy batch reactor charged with 0.546 g of 5 wt% Ru/C (Johnson Matthey, type 5R600), reduced at 300 °C then pre-reduced in the reactor at 100 °C; substrate = 41.5 g of 10–20 wt% aqueous oxalic acid; stir rate = 400 rpm; pressure = 100 bar H2; temperature = 75 °C.

temperatures compared to what was suggested by Santos *et al.*, or used in the examples of Lange *et al.*[42,43] Whilst the reduction of the reaction temperature lowered the production of volatiles, the production of acetic acid could not be avoided. To achieve high activity, we recommend the reduction of ruthenium-based catalysts at temperatures of 350–400 °C followed by an *in situ* pre-reduction step. The selectivity towards glycolic acid or ethylene glycol were insensitive towards changes in catalyst or metal loading, hydrogen pressure and reactant concentration. Although the reaction of oxalic acid towards glycolic acid was preferred over the reduction of glycolic acid to ethylene glycol, the formation of ethylene glycol can only be prevented if not more than 50–70% of the oxalic acid is converted. The formation of Acetic acid could not be prevented with this catalyst and was occurring at a significant rate of around 10% even at lower reaction temperatures. Overall, we conclude that the most suitable reaction conditions are 75 °C, 80 bar H_2, an oxalic acid concentration of 5 wt% and pre-reduction of the catalyst in H_2 *ex situ* at 350 °C for 3 h and *in situ* at 200 °C for 2 h. We translated those results to use them in the high-throughput batch reactor system Batchington and used them for our catalyst screening.

Explorative catalyst screening

For the initial exploration of a new catalyst for the oxalic acid to glycolic acid reduction, we chose to produce catalysts known as well-functioning in reduction reactions. We chose to test three catalysts reported for the reduction of dicarboxylic acids which we synthesised following the protocol of the original publications (details ESI 3.1–3.3†).[56,59,61] In addition, we synthesised catalysts that encapsulate ruthenium nanoparticles in polymeric dopamine structures; catalysts with ruthenium dimers as active sites on carbon which were synthesized with (benzene) ruthenium dichloride dimer as a precursor, and two different MXene catalysts with the chemical formula: Ti_3AlC_2 and Ti_2AlC (details ESI 3.4–3.5†).[68,69]

We tested all catalysts using optimised reaction conditions in a Batchington system at 75 °C, 80 bar H_2, 5 wt% oxalic acid and reaction times of 2, 4 and 6 hours (details ESI 4.3†). We analysed the contents of the liquid products the with HPLC after filtration.[62] As shown in Fig. 9, unfortunately, none of the catalysts we tested converted oxalic acid effectively and the selectivity to glycolic acid was poor. The three copper-magnesium, indium oxide, and nickel-iron catalysts showed 40–55% loss in carbon balance potentially caused by adsorption of oxalic acid on the catalyst. Overall, the poor performance of these catalysts leads us to develop new catalysts.

The most active metal for oxalic acid hydrogenation

Although ruthenium has proven suitable for oxalic acid reduction, we aimed to systematically test other metals and eventually substitute ruthenium with a metal of lower cost and higher availability. We synthesized new catalysts with 5 wt% ruthenium, scandium, nickel, copper, cobalt, platinum, palladium, and rhenium on carbon support using wet impregnation (details ESI 3.7†) and tested them in the Batchington reactor (details ESI 4.4†). With ICP-OES measurements we confirmed that the theoretical and actual metal loading of the catalysts is in close agreement. The results for alternative active metals (Fig. 10) show that only ruthenium and palladium reduced oxalic acid to glycolic acid. The ruthenium catalyst led to a conversion of 73% after 6 h at 125 °C with a 90% glycolic acid selectivity and 10% acetic acid production. Palladium based catalysts are active in the hydrogenation of di-acids such as succinic acid selectively to γ-butyrolactone leading primarily to the respective hydroxy acids at 160–200 °C.[70–73] Given the unusually high reactivity of the oxalic acid, we tested the Pd/C based system in the temperature range of 75–125 °C. The results in Fig. 10 show that carbon-supported palladium shows no activity at 75 °C. Increasing the temperature to 100 °C and 125 °C led to a loss in carbon mass balance and the formation of 5% glycolic acid. Samples collected from reactors containing the rhenium catalyst retained a black colour after filtration with the syringe filters. No reaction product is visible for the rhenium-catalysed reaction which indicates leaching of rhenium in the acidic reaction environment. We conclude that ruthenium is the only suitable metal for oxalic acid reduction.

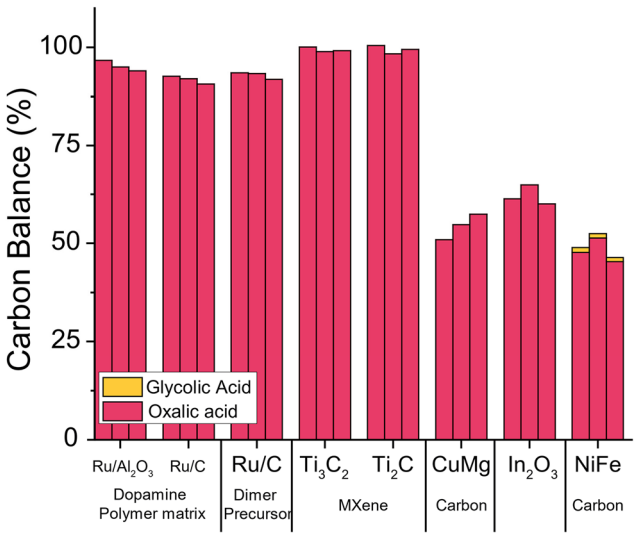

Fig. 9 Poor performance of literature-based catalysts for the reduction of oxalic acid to glycolic acid expressed as carbon balance of dissolved compounds after reaction obtained by HPLC. Detailed composition of the catalyst: Ru/Al_2O_2 polymer: synthesised in one pot from Al_2O_3, ruthenium chloride precursor and dopamine; Ru/C polymer: synthesised in one pot from carbon (Norit SX-1), ruthenium chloride precursor and dopamine; Ru/C dimer: produced from (benzene)ruthenium dichloride dimer impregnated on Norit 1-SX carbon; Ti_3C_2 MXene: synthesised by exfoliation of MAX phase; Ti_2C MXene; synthesised by exfoliation of MAX phase; CuMg/C: In_2O_3: synthesised from indium nitrate; NiFe/C: synthesised from nickel, iron and carbon precursors in one pot followed by pyrolysis; all reactions were performed using a batchington parallel reactor system. conditions: temperature = 75 °C, pressure = 80 bar H_2H, substrate = oxalic acid (5 wt%) in demineralized water (2 mL), catalyst/support loading = 50 mg (pre-reduced in H_2 *ex situ* at 350 °C for 3 h and *in situ* at 200 °C for 2 h), stir rate = 800 rpm, time = 2, 4 and 6 hours.

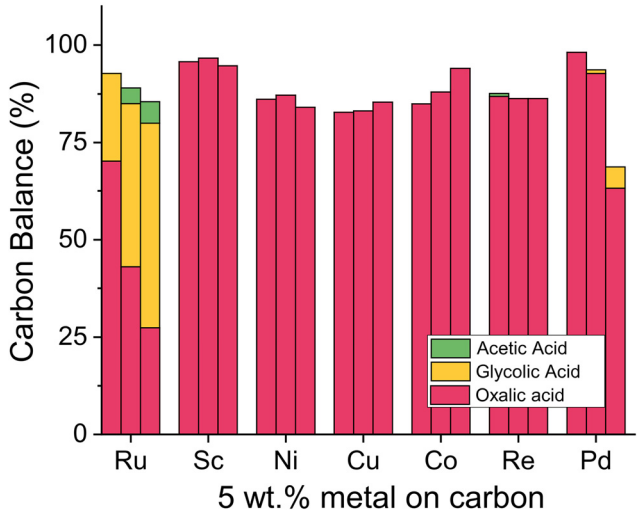

Fig. 10 Carbon balance in oxalic acid reduction reaction with different metals at 2-, 4- and 6-hours reaction time. Metals include ruthenium (Ru), scandium (Sc), nickel (Ni), copper (Cu), cobalt (Co), rhenium (Re), and palladium (Pd) loaded on the same carbon support. Carbon balance data was obtained by HPLC. All reactions were performed using a batchington parallel batch reactor. All reactions were performed using a batchington parallel reactor system. Conditions: temperature = 75 °C, pressure = 80 bar H_2H, substrate = oxalic acid (5 wt%) in demineralized water (2 mL), Catalyst/Support Loading = 50 mg (pre-reduced in H_2 *ex situ* at 350 °C for 3 h and *in situ* at 200 °C for 2 h), stir rate = 800 rpm, time = 2, 4 and 6 hours. For the palladium catalyst, all reaction times are 6 h but temperatures have been varied (75 °C, 100 °C and 125 °C).

The most suitable support for ruthenium based catalysts

A heterogeneous catalyst consists of two main components: the active metallic species (which catalyses the reaction on its surface) and the support material. The latter usually features a high surface area, is porous and can fulfil various functions: it allows the distribution of the active metal as small particles to increase the active area, it prevents sintering of the active metal to larger particles during the reaction, it helps adsorb and desorb reactants. In some cases, it even acts as a part of the catalytic system itself and facilitates parts of the reaction or transport of intermediates. In the proposed mechanism for the oxalic acid hydrogenation to glycolic acid by Santos *et al.*, hydrogen is split on the carbon surface and transported to the active ruthenium species (Fig. 2).[43] Due to the active role of carbon we decided to compare various commercially available carbons. Carbon supports are often obtained by pyrolyzing a diverse mix of molecules and therefore contain more elements than carbons and vary drastically in their structure. For our test, we include carbon supplied by Norit Co. (SX Plus, R1 extra, RO-0.8, ROW-0.8, DARCO G60), Pica USA (PICATAL) and Fisher chemicals (FISHER). We prepared catalysts with 5 wt% of ruthenium *via* incipient wetness impregnation (details ESI 3.6†) and tested them at 75 °C in the 100 mL Hastelloy reactor (details ESI 4.5†) as a reference we used a commercial catalyst from Johnson Matthey (JM, 5R600).

The results of the catalyst screening are shown in Fig. 11 where the oxalic acid conversion (11A) and the calculated product distribution (11B) are plotted against the type of carbon used in the catalyst synthesis. Ethylene glycol was always formed at oxalic acid conversions above 70%. The catalysts with the highest conversion after six hours were Norit R1-extra (91%) followed by Norit RO-0.8 (88%), and Picatal (86%). However, these catalysts also had the highest selectivity towards acetic acid (9.8%, 9.6%, and 9.9%). The catalysts prepared with Fisher and Darco G-60 showed similar selectivity towards acetic acid (9.7% and 8.1%) but were less active. The most promising supports in our study were Norit SX-Plus and Norit ROW-0.8 as we could reduce the production of acetic acid by 43% compared to the three most active catalysts (acetic acid selectivity was 5.6% for Norit SX-Plus and 5.7% for Norit ROW-0.8). This, unfortunately, came at the cost of activity with maximum conversions of 49% for Norit ROW-0.8 and 61% for Norit SX-Plus. As our primary goal was to find a more selective catalyst, we decided to continue developing a catalyst using Norit SX-Plus as carbon support. Subsequently, we tested the influence of the particle size of the carbon. We synthesised catalysts with different mesh sizes of Norit SX-Plus: a non-uniform mesh size (as used in the comparison of different carbon types), a particle size of 200–325 mesh, and a particle size of 300–450 mesh. Fortunately, using a defined size of 200–325 mesh increases the conversion from 61 to 80% whilst maintaining the low selectivity towards acetic acid. Therefore, using suitable carbon support, already allowed us to decrease the acetic acid production with only small losses in overall catalyst activity. The dedicated modification of the surface moieties of the carbon support by introducing e.g acid functionalities presents an opportunity for further improvement in the future.

We expanded the scope of supports and prepared ruthenium catalyst with $Ti_3(Al_{0.8}Sn_{0.2})C_2$ MAX phases and metal oxides including TiO_2, Al_2O_3, MgO, CeO_2 and ZrO_2 as supports. We tested the activity of the support without active metal and then prepared catalysts with a 5 wt% loading of ruthenium using wet impregnation followed by calcination and reduction in a hydrogen atmosphere (details ESI 3.9†). All catalysts were then tested at 75 °C in the Batchington reactor (details ESI 4.6†).[62] For supports without ruthenium, we observed no conversion (Fig. S1†). The loss in carbon balance for the MgO support could be attributed to the adsorption of oxalic acid on the support in a dedicated control experiment (Fig. S2†).

The addition of ruthenium produced active catalysts and even the 5 wt% Ru/MgO catalyst converted some oxalic acid to glycolic acid (Fig. 12). The highest conversions of oxalic acid were achieved with 5 wt% Ru/C (72.5%), 5 wt% Ru/TiO_2 (74.4%), and 5 wt% Ru/$Ti_3(Al_{0.8}Sn_{0.2})C_2$ MAX-Phase (89.6%). Other catalysts had a notably lower conversion with 61% for 5 wt% Ru/CeO_2, 43% for 5 wt% Ru/ZrO_2 and the lowest conversion of 17% when using 5 wt% Ru/Al_2O_3. The selectivity towards glycolic acid decreased with increasing reaction time for 5 wt% Ru/C, 5 wt% Ru/TiO_2, 5 wt% Ru/$Ti_3(Al_{0.8}Sn_{0.2})C_2$

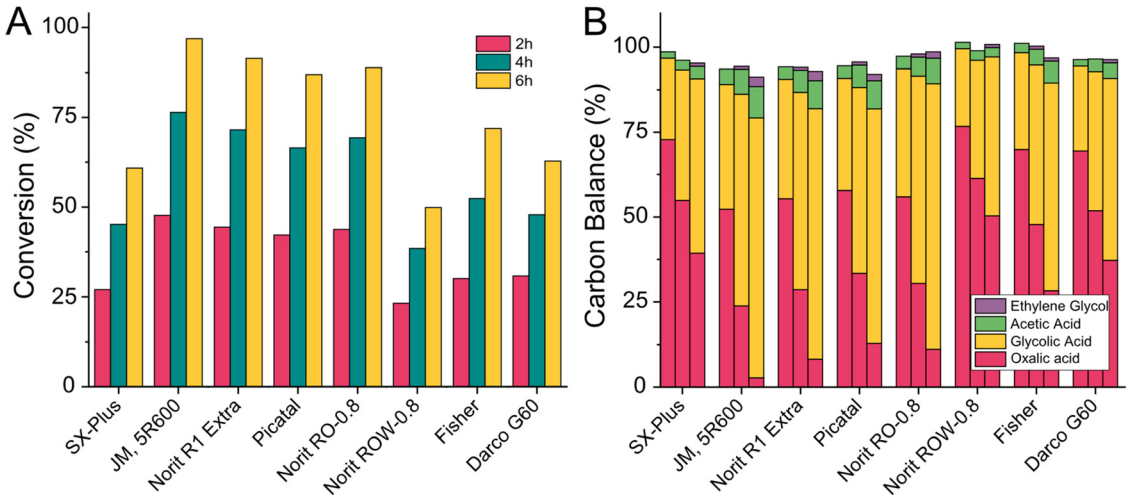

Fig. 11 Influence of carbon support in ruthenium catalysts on: (A) oxalic acid conversion and (B) carbon balance of dissolved compounds after reaction obtained by liquid chromatography (LC). As a comparison, we added the commercially available catalyst JM, 5R600 (5 wt% Ru on Carbon). All reactions were performed using a 100 mL all Hastelloy batch reactor charged with 1.125 g of catalyst reduced at 300 °C for 3 h then pre-reduced in the reactor at 100 °C. Conditions: substrate = 41.5 g of 10 wt% aqueous oxalic acid; stir rate = 400 rpm; pressure = 100 bar H_2; temperature = 75 °C; reaction time = 6 hours (shown are 2, 4 and 6 hours).

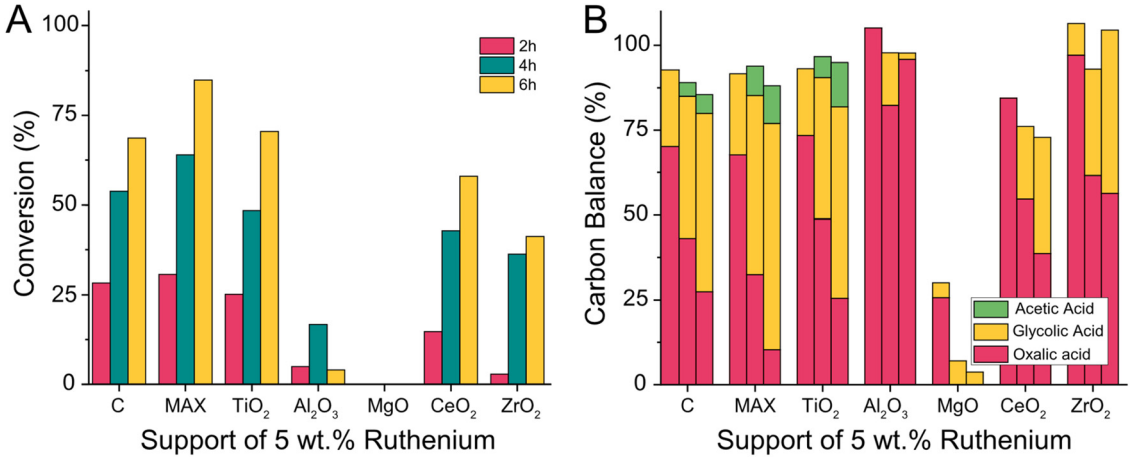

Fig. 12 Performance of ruthenium catalysts with different supports for the reduction of oxalic acid expressed in: (A) oxalic acid conversion and (B) carbon balance of dissolved compounds after reaction obtained by liquid chromatography (LC). All reactions were performed using a batchington parallel batch reactor. Temperature = 75 °C, pressure = 80 bar H_2H, substrate = oxalic Acid (5 wt%) in demineralized water (2 mL), catalyst/support loading = 50 mg (pre-reduced in H_2 *ex situ* at 350 °C for 3 h and *in situ* at 200 °C for 2 h), Stir rate = 800 rpm, time = 2, 4 and 6 hours.

MAX-Phase and 5 wt% Ru/CeO_2 as more acetic acid was formed with time (Fig. 12B). The least acetic acid at high conversion was formed when using the Ru/C catalyst whilst the acetic acid formation was more pronounced with the Ru/MAX and Ru/TiO_2 catalysts. The carbon balance was above 85% for most catalysts, except for 5 wt% Ru/MgO and 5 wt% Ru/CeO_2. In the case of 5 wt% Ru/MgO, this is caused by the absorption of oxalic acid as described above. In the case of 5 wt% Ru/CeO_2, we did not observe adsorption earlier and therefore assume the pronouncement of the undesired formation of volatiles when CeO_2 is used as a support.

Unfortunately, oxalic acid can not only be converted by stable supported metal particles, but also by non-supported metal particles leached from the catalyst surface into the reactant solution. Whilst the measured reaction outcome is the same, the leached metal is lost after the reaction and therefor the catalysts degrades over time. We use ICP-OES to detect if any ruthenium leached from the catalyst during the reaction (Table 2). We could show, that only the zirconia based catalyst leached significantly (up to 4.5% of all Ruthenium after 6 h) with a clear correlation of reaction time and leaching of ruthenium. The carbon, alumina and titania supported catalysts showed very little leaching of maximum 0.39% and the leaching did not increase with reaction times. Hence we attribute their catalytic activity to the supported metal particles.

We used physisorption and XRD measurements to gain insight into our catalysts' surface area, pore structure (Table 3) and the crystal structure of ruthenium particles (Fig. 13). The surface area of pristine supports was A_{BET} = 865 m^2 g^{-1} for the carbon, 101 m^2 g^{-1} for TiO_2 and only 0.59 m^2 g^{-1} for the $Ti_3(Al_{0.8}Sn_{0.2})C_2$ MAX phase. Interestingly the addition of ruthenium had a different effect for each support. Whilst the surface area increased for carbon and $Ti_3(Al_{0.8}Sn_{0.2})C_2$ MAX phase supports and the pore volume stayed about the same, this was not the case for TiO_2. Ruthenium blocks the pores when applied to TiO_2 which led to a reduction in surface area. Albeit the surface area of the three catalysts greatly differs, they perform equally well in terms of conversion and selectivity. On the $Ti_3(Al_{0.8}Sn_{0.2})C_2$ MAX-phase support, the ruthenium particles were visible in XRD, whereas for carbon and titania, little to no ruthenium particles were visible. The surface area of the supports did not affect the performance of the different catalysts. Possibly, the acidity of the support has more effect since, for example, the relatively basic Al_2O_3 performed significantly worse. Carbon supports are known to be more stable than inorganic supports in aqueous processes at low pH. Also metal recovery from spent catalysts is simple for C-based catalysts (burning away the carbon). Overall, carbon was the most suitable support as it combines high activity with the lowest formation of acetic acid.

Table 2 Measurement of ruthenium content in reaction solutions with ICP-OES after oxalic acid hydrogenation in Batchington parallel batch reactor. Temperature = 75 °C, Pressure = 80 bar H_2H, Substrate = Oxalic Acid (5 wt%) in demineralized water (2 mL), Catalyst/Support Loading = 50 mg (pre-reduced in H_2 *ex situ* at 350 °C for 3 h and *in situ* at 200 °C for 2 h), Stir rate = 800 rpm, Time = 2, 4 and 6 hours

Catalyst	Leached metal after: 2 h Reaction	4 h Reaction	6 Reaction
5 wt% Ru/C	0,39%	0,29%	0,27%
5 wt% Ru/Al_2O_3	0,21%	0,31%	0,13%
5 wt% Ru/TiO_2	0,11%	0,10%	0,06%
5 wt% Ru/ZrO	2.0%	3,3%	4.5%

Table 3 Measurement of surface area, pore volume and pore radius of different supports and ruthenium catalyst using nitrogen adsorption (BET) measurements. The surface area and pore radius were determined by using nitrogen as an adsorbate

Catalyst	Surface area (m^2 g^{-1})	Pore volume (cm^3 g^{-1})	Pore radius (nm)
Carbon	864.88	0.68	1.39
Ru/C	1030.16	0.71	1.38
$Ti_3(Al_{0.8}Sn_{0.2})C_2$ MAX	0.59	0.02	5.62
Ru/$Ti_3(Al_{0.8}Sn_{0.2})C_2$ MAX	10.78	0.03	5.53
TiO2	101.38	0.73	14.47
Ru/TiO2	14.60	0.16	22.48

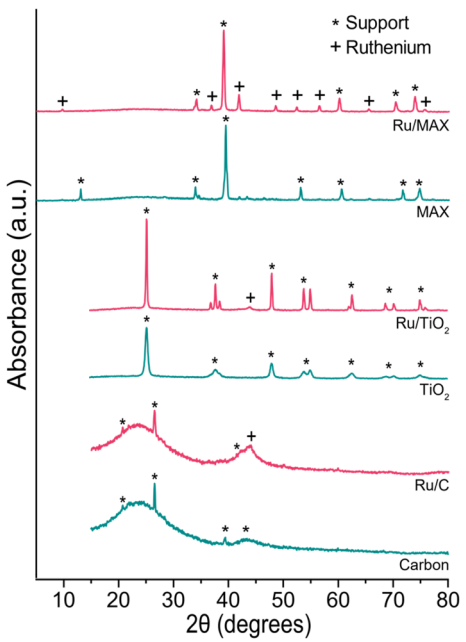

Fig. 13 X-ray diffraction (XRD) spectra of $Ti_3(Al_{0.8}Sn_{0.2})C_2$ MAX-phase and Ru/$Ti_3(Al_{0.8}Sn_{0.2})C_2$ MAX (5 wt%), TiO_2 and Ru/TiO_2 (5 wt%), Carbon and Ru/Carbon (5 wt%). The diffractograms were measured from 5 or 15 to 80 degrees with a scan rate of 1°/minute. The diffraction peaks were assigned using a spectral database within the Rigaku PDXL software.

Commercial catalyst

Having established that the combination of ruthenium as active metal and carbon as a support are most desirable, we turned to commercially available Ru/C catalysts which are widely available. Avoiding the need to produce a bespoke catalyst for a process such as in the OCEAN project is desirable as it reduces the risk and time required to establish large-scale catalyst production. We chose a low reaction temperature of 75 °C to observe the kinetic behaviour of the catalysts over six hours. We tested catalysts from commercial suppliers with 5 wt%, 7.5 wt% or 10 wt% ruthenium supported on carbon or alumina (Table S3†) at 75 °C in a 100 mL Hastelloy reactor (details ESI 4.7†).

We observe the same trends for all tested catalysts as shown in Fig. 14. During the heating of the reactor (time before 0 h) already some oxalic acid was converted to glycolic acid. Over the time of the reaction, the conversion increased constantly for all catalysts, except for the catalyst using alumina as support. The 5% Ru/Al_2O_3 catalyst was already deactivated after 4 hours as the conversion started to stagnate. Higher loadings of ruthenium lead to a higher conversion except for Johnson Matthey C-11252, a 5 wt% Ru/C catalyst, which showed activity comparable to the catalysts with higher loadings. The highest yield of glycolic acid was 74.6% and was achieved using the catalyst with 7.5 wt% ruthenium loading. The production of ethylene glycol only reached 7% and was caused by the over-reduction of glycolic acid. As higher loadings of ruthenium lead to higher conversion, also ethylene glycol production increased for those catalysts. We chose the most suitable catalyst based on the overall carbon mass balance. The highest carbon losses occurred with higher metal loadings and reached up to 21% for the 10 wt% Ru/C catalyst. The overall best catalyst was the 5 wt% Ru/C Johnson Matthey

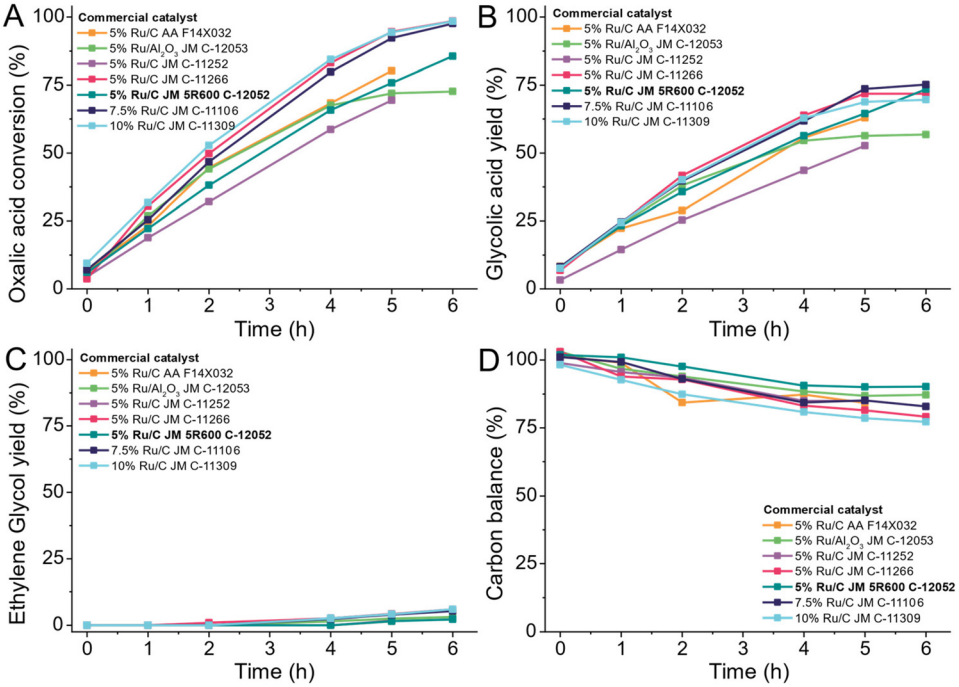

Fig. 14 Influence of commercial catalyst on the reduction of 5% oxalic acid in aqueous feed on (A) oxalic acid conversion, (B) glycolic acid yield, (C) ethylene glycol yield, and (D) carbon balance. All reactions were performed using a 100 mL all Hastelloy batch reactor charged with 1.175 g of catalyst reduced at 300 °C for 3 h then pre-reduced in the reactor at 100 °C; Substrate: 42 g of 5% oxalic acid in water; Stir rate: 400 RPM; pressure: 100 bar H_2; temperature 75 °C.

type 5R600. It shows a consistent increase in conversion, has the highest selectivity for glycolic acid and didn't show any sign of deactivation. Most notably it led to the highest overall carbon balance of all tested catalysts.

Bi-metallic ruthenium catalyst

All tested commercial Ru/C catalysts produce 7–15% of Acetic acid and ethylene glycol at high oxalic acid conversion levels. To avoid these reactions, we started adding a second metal to the ruthenium catalyst as a promoter by adding 1 wt% of either tin, bismuth, palladium, rhenium, platinum, gold, or antimony by co-impregnation (details ESI 3.8†). For comparison, we also synthesised a singular monometallic 5 wt% Ru/C and calcined and pre-reduced all catalysts (details ESI 3.9†) before testing them in the 100 mL Hastelloy reactor at 75 °C (details ESI 4.14†).

Based on the limited number of studied promoters, we observe the existence of three distinct types of promotion (Fig. 15). In case A (promotor being Re, Pt and Au), the resulting catalyst shows a similar reaction rate (no change in the

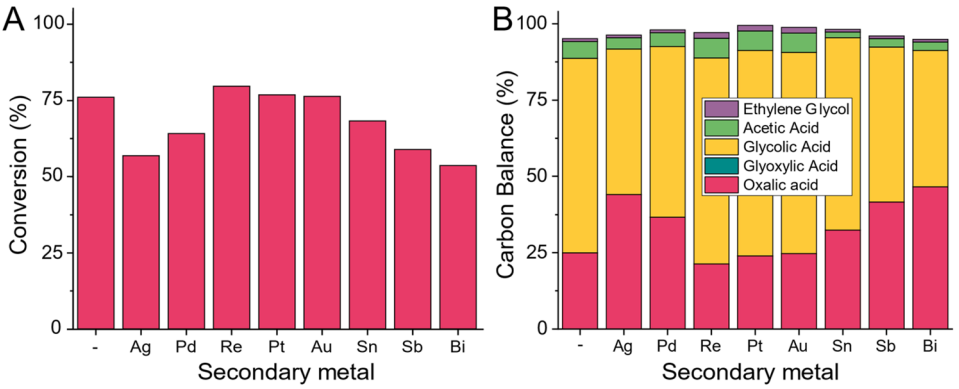

Fig. 15 Performance bimetallic catalysts with ruthenium as the primary metal in oxalic acid reduction expressed as (A) conversion and (B) carbon balance. Catalysts were prepared by co-impregnating carbon with 5 wt% of Ruthenium and 1 wt% of silver (Ag), palladium (Pd), rhenium (Re), platinum (Pt), gold (Au), tin (Sn), antimony (Sb) or bismuth (Bi). All reactions were performed in a 100 mL Hastelloy batch reactor; samples were quantified using liquid chromatography (LC). Conditions during reactions: 2 g of catalyst, reduced at 300 °C then pre-reduced in the reactor at 100 °C; substrate = 41.5 g of 10 wt% aqueous oxalic acid; stir rate = 400 rpm; pressure = 100 bar H2; temperature = 75 °C; reaction time = 6 hours.

conversion level) but a small improvement in both the selectivity to glycolic acid and a higher carbon mass balance. For these three promoters, no improvement in the acetic acid level was observed. For modifiers of type B (Pd and Ag), the rate reduction (lower conversion) was accompanied by some reduction in the acetic acid. The most interesting additive is tin. At the current 1 wt% promotion level, some minor rate reduction (drop-in conversion from 75.2% to 67.5%) was combined with the dramatic reduction in the acetic acid level – from the 7.8% observed for the unpromoted catalyst, the acetic acid level with the 5 wt% Ru-1 wt% Sn/C catalyst was reduced to 3.1%. Along with this very promising result, both the overall carbon balance and the selectivity to glycolic acid were also improved – the CB was increased from 95.1% to 98.2% while the glycolic acid selectivity was increased from 83.9% to 92.9%. This does not come as a surprise as the benefits of adding tin to ruthenium based catalysts have been described before.[40–46] In bi- or multi-metallic catalysts, one should differentiate between the two metals forming alloys or being present as separate metal and metal oxides species which can benefit the reaction due to the geometric or electronic effects. For Ruthenium and Tin systems both have been proposed and thus we aim a in-depth investigation of the role on tin addition in this case.[46] Given this very encouraging result, we decided to develop a new catalyst system consisting of carbon as support, ruthenium as main metal and tin as secondary metal which we will be discussing in a upcoming paper.

Conclusions

In conclusion, we could show, that oxalic acid can be efficiently reduced to glycolic acid at reaction temperatures below 100 °C and high selectivity using ruthenium-carbon catalysts. During our extensive screening of catalysts and reaction conditions tested different active metals, supports, and found ruthenium on carbon most active and selective. Commercially available Ru/C catalysts all caused the formation of ethylene glycol and acetic acid no matter the reaction conditions. When varying the reaction temperature, we showed that volatile and acetic acid production strongly increased above 100 °C. The ideal reaction temperature was 75 °C. The conversion increased linearly with catalyst loading and metal loading, the selectivity towards ethylene glycol, acetic acid and glycolic acid was not affected. Hence, lower reaction rates could be compensated with higher catalyst loading (7.5 wt%) and hydrogen pressures (100 bar). The reactant concentration did not affect the selectivity of the reaction in the tested range (5–20 wt% oxalic acid in water). *Ex situ* (350 °C) and *in situ* (pre)reduction (100 °C) of the catalyst increased its activity without affecting selectivity. At last, we decided to develop a bespoke catalyst to improve avoid acetic acid and ethylene glycol production. We added eight different metals as a promoter to the ruthenium-based catalyst. Some did not affect the activity but slightly improved selectivity towards glycolic acid and the overall carbon balance (Re, Pt, and Au). Others reduced the activity and slightly reduced acetic acid production (Ag and Pd). The best improvement was achieved with tin as a promoter which reduced the acetic acid production by 61%.

Overall, our results show, that the direct reduction of oxalic acid to glycolic acid can be achieved at high selectivity and low temperatures with bimetallic ruthenium-tin catalysts for a better and more sustainable process which is competitive with current commercial pathways to glycolic acid when using sustainable feedstocks. We explored the boundaries and formed the foundation for the development of new catalysts for this reaction which is a crucial step in the conversion of CO_2 to valuable chemicals and polymers.

Conflicts of interest

There are no conflicts to declare.

Acknowledgements

This project has received funding from the European Union's Horizon 2020 research and innovation program under grant agreement No 767798. Funding for Seton Hall University was provided by Liquid Light Inc. We like to thank Thierry K. Slot and Maria Ronda Lloret, Pieter Laan and Ihsan Amin for their contributions to synthesise catalyst following novel concepts. Thierry K. Slot and Maria Ronda Lloret provided MXenes and MAX phase materials for this work. Pieter Laan helped with providing the knowledge to prepare the dimeric catalysts. Ihsan Amin provided the knowledge and recipe to prepare the polymeric catalysts. Alan Smith provided insight in the current glycolic acid production and helped with the cost price estimates.

References

1 P. G. Levi and J. M. Cullen, Mapping Global Flows of Chemicals: From Fossil Fuel Feedstocks to Chemical Products, *Environ. Sci. Technol.*, 2018, **52**(4), 1725–1734, DOI: **10.1021/acs.est.7b04573**.

2 P. Styring, E. A. Quadrelli and K. Armstrong, Carbon Dioxide Utilisation. In *Carbon Dioxide Utilisation: Closing the Carbon Cycle: First Edition*, Elsevier, 2015, pp 237–272. DOI: **10.1016/C2012-0-02814-1**.

3 I. A. G. Wilson and P. Styring, Why Synthetic Fuels Are Necessary in Future Energy Systems, *Front. Energy Res.*, 2017, **5**(19), 1–10, DOI: **10.3389/fenrg.2017.00019**.

4 T. Keijer, V. Bakker and J. C. Slootweg, Circular Chemistry to Enable a Circular Economy, *Nat. Chem.*, 2019, **11**(3), 190–195, DOI: **10.1038/s41557-019-0226-9**.

5 C. Ampelli, S. Perathoner and G. Centi, CO 2 Utilization: An Enabling Element to Move to a Resource- and Energy-Efficient Chemical and Fuel Production, *Philos. Trans. R. Soc., A*, 2015, **373**(2037), 20140177, DOI: **10.1098/rsta.2014.0177**.

6 F. D. Meylan, V. Moreau and S. Erkman, CO2 Utilization in the Perspective of Industrial Ecology, an Overview, *J. CO2 Util.*, 2015, **12**, 101–108, DOI: 10.1016/j.jcou.2015.05.003.
7 A. Kätelhön, R. Meys, S. Deutz, S. Suh and A. Bardow, Climate Change Mitigation Potential of Carbon Capture and Utilization in the Chemical Industry, *Proc. Natl. Acad. Sci. U. S. A.*, 2019, **166**(23), 11187–11194, DOI: 10.1073/pnas.1821029116.
8 G. Centi, G. Iaquaniello and S. Perathoner, Chemical Engineering Role in the Use of Renewable Energy and Alternative Carbon Sources in Chemical Production, *BMC Chem. Biol.*, 2019, **1**(1), 5, DOI: 10.1186/s42480-019-0006-8.
9 S. Perathoner and G. Centi, Catalysis for Solar-Driven Chemistry: The Role of Electrocatalysis, *Catal. Today*, 2019, **330**, 157–170, DOI: 10.1016/j.cattod.2018.03.005.
10 G. Centi, E. A. Quadrelli and S. Perathoner, Catalysis for CO2 Conversion: A Key Technology for Rapid Introduction of Renewable Energy in the Value Chain of Chemical Industries, *Energy Environ. Sci.*, 2013, **6**(6), 1711–1731, DOI: 10.1039/c3ee00056.
11 E. A. Quadrelli, G. Centi, J.-L. Duplan and S. Perathoner, Carbon Dioxide Recycling: Emerging Large-Scale Technologies with Industrial Potential, *ChemSusChem*, 2011, **4**(9), 1194–1215, DOI: 10.1002/cssc.201100473.
12 C. Hepburn, E. Adlen, J. Beddington, E. A. Carter, S. Fuss, N. Mac Dowell, J. C. Minx, P. Smith and C. K. Williams, The Technological and Economic Prospects for CO2 Utilization and Removal, *Nature*, 2019, **575**(7781), 87–97, DOI: 10.1038/s41586-019-1681-6.
13 O. S. Bushuyev, P. De Luna, C. T. Dinh, L. Tao, G. Saur, J. van de Lagemaat, S. O. Kelley and E. H. Sargent, What Should We Make with CO2 and How Can We Make It?, *Joule*, 2018, **2**(5), 825–832, DOI: 10.1016/j.joule.2017.09.003.
14 Oxalic acid from CO2 using Eletrochemistry At demonstratioN scale | OCEAN Project | H2020 | CORDIS | European Commission https://cordis.europa.eu/project/id/767798 (accessed Feb 4, 2020).
15 E. Palm, L. J. Nilsson and M. Åhman, Electricity-Based Plastics and Their Potential Demand for Electricity and Carbon Dioxide, *J. Cleaner Prod.*, 2016, **129**, 548–555, DOI: 10.1016/j.jclepro.2016.03.158.
16 U. Wöhler, F. Die and S. Der, *Polytech. J.*, 1824, **15**(33), 177–184.
17 E. Schuler, M. Demetriou, N. R. Shiju and G.-J. M. Gruter, Towards Sustainable Oxalic Acid from CO 2 and Biomass, *ChemSusChem*, 2021, **14**(18), 3636–3664, DOI: 10.1002/cssc.202101272.
18 V. M. A. Murcia, R.-J. van Putten and G.-J. M. Gruter, The Potential of Oxalic – and Glycolic Acid Based Polyesters (Review). Towards CO2 as a Feedstock (Carbon Capture and Utilization – CCU), *Eur. Polym. J.*, 2019, **119**, 445–468, DOI: 10.1016/j.eurpolymj.2019.07.036.
19 Transparency Market Research. Glycolic Acid Market - Global Industry Analysis, Size, Share, Growth, Trends, and Forecast, 2019–2027; 2019.
20 A. F. Kurniawan, I. Ma'rufi and A. D. P. Sujoso, Hydroxycarboxylic Acids, Aliphatic, *Ullmann's Encycl. Ind. Chem.*, 2012, **18**, 481–492, DOI: 10.1002/14356007.a13.
21 D. J. Loder, Process for Manufacture of Glycolic Acid. US2152852, 1939.
22 D. Zhao, T. Zhu, J. Li, L. Cui, Z. Zhang, X. Zhuang and J. Ding, Poly(Lactic-Co-Glycolic Acid)-Based Composite Bone-Substitute Materials, *Bioact. Mater.*, 2021, **6**(2), 346–360, DOI: 10.1016/J.BIOACTMAT.2020.08.016.
23 S. Yunhai, S. Houyong, C. Haiyong, L. Deming and L. Qinghua, Synergistic Extraction of Glycolic Acid from Glycolonitrile Hydrolysate, *Ind. Eng. Chem. Res.*, 2011, **50**(13), 8216–8224, DOI: 10.1021/ie200445n.
24 B.-Y. Yu, C.-Y. Chung and I.-L. Chien, Development of a Plant-Wide Dimethyl Oxalate (DMO) Synthesis Process from Syngas: Rigorous Design and Optimization, *Comput. Chem. Eng.*, 2018, **119**, 85–100, DOI: 10.1016/j.compchemeng.2018.08.025.
25 E. Göktürk, A. G. Pemba and S. A. Miller, Polyglycolic Acid from the Direct Polymerization of Renewable C1 Feedstocks, *Polym. Chem.*, 2015, **6**(21), 3918–3925, DOI: 10.1039/C5PY00230C.
26 P. K. Samantaray, A. Little, D. M. Haddleton, T. McNally, B. Tan, Z. Sun, W. Huang, Y. Ji and C. Wan, Poly(Glycolic Acid) (PGA): A Versatile Building Block Expanding High Performance and Sustainable Bioplastic Applications, *Green Chem.*, 2020, **22**(13), 4055–4081, DOI: 10.1039/D0GC01394C.
27 X. Zhou, M. Zha, J. Cao, H. Yan, X. Feng, D. Chen and C. Yang, Glycolic Acid Production from Ethylene Glycol via Sustainable Biomass Energy: Integrated Conceptual Process Design and Comparative Techno-Economic-Society-Environment Analysis, *ACS Sustainable Chem. Eng.*, 2021, **9**(32), 10948–10962, DOI: 10.1021/ACSSUSCHEMENG.1C03717/SUPPL_FILE/SC1C03717_SI_001.PDF.
28 J. G. Rosenboom, R. Langer and G. Traverso, Bioplastics for a Circular Economy, *Nat. Rev. Mater.*, 2022, **7**(2), 117–137, DOI: 10.1038/s41578-021-00407-8.
29 N. Escobar and W. Britz, Metrics on the Sustainability of Region-Specific Bioplastics Production, Considering Global Land Use Change Effects, *Resour., Conserv. Recycl.*, 2021, **167**, 105345, DOI: 10.1016/J.RESCONREC.2020.105345.
30 J. P. Lange, Performance Metrics for Sustainable Catalysis in Industry, *Nat. Catal.*, 2021, **4**(3), 186–192, DOI: 10.1038/s41929-021-00585-2.
31 M. Tamura, Y. Nakagawa and K. Tomishige, Recent Developments of Heterogeneous Catalysts for Hydrogenation of Carboxylic Acids to Their Corresponding Alcohols, *Asian J. Org. Chem.*, 2020, **9**(2), 126–143, DOI: 10.1002/ajoc.201900667.
32 J. E. Carnahan, T. A. Ford, W. F. Gresham, W. E. Grigsby and G. F. Hager, Ruthenium-Catalyzed Hydrogenation of Acids to Alcohols, *J. Am. Chem. Soc.*, 1955, **77**(14), 3766–3768, DOI: 10.1021/ja01619a025.
33 A. Primo, P. Concepción and A. Corma, Synergy between the Metal Nanoparticles and the Support for the

Hydrogenation of Functionalized Carboxylic Acids to Diols on Ru/TiO2, *Chem. Commun.*, 2011, **47**(12), 3613, DOI: 10.1039/c0cc05206j.

34 D. Sun, S. Sato, W. Ueda, A. Primo, H. Garcia and A. Corma, Production of C4 and C5 Alcohols from Biomass-Derived Materials, *Green Chem.*, 2016, **18**(9), 2579–2597, DOI: 10.1039/C6GC00377J.

35 J. E. Carnahan, T. A. Ford, W. F. Gresham, W. E. Grigsby and G. F. V. Hager, Ruthenium-Catalyzed Hydrogenation of Acids to Alcohols, *J. Am. Chem. Soc.*, 1955, **77**(14), 3766–3768, DOI: 10.1021/ja01619a025.

36 J. Zhu, Y. Ye, Y. Tang, L. Chen and K. Tang, Efficient Hydrogenation of Dimethyl Oxalate to Ethylene Glycol via Nickel Stabilized Copper Catalysts, *RSC Adv.*, 2016, **6**(112), 111415–111420, DOI: 10.1039/C6RA23474G.

37 H. T. Teunissen and C. J. Elsevier, Ruthenium Catalysed Hydrogenation of Dimethyl Oxalate to Ethylene Glycol, *Chem. Commun.*, 1997, (7), 667–668, DOI: 10.1039/a700862.

38 U. Matteoli, M. Bianchi, G. Menchi, P. Frediani and F. Piacenti, Hydrogenation of Dimethyl Oxalate in the Presence of Ruthenium Carbonyl Carboxylates: Ethylene Glycol Formation, *J. Mol. Catal.*, 1985, **29**(2), 269–270, DOI: 10.1016/0304-5102(85)87009-7.

39 P. A. Dub and T. Ikariya, Catalytic Reductive Transformations of Carboxylic and Carbonic Acid Derivatives Using Molecular Hydrogen, *ACS Catal.*, 2012, **2**(8), 1718–1741, DOI: 10.1021/cs300341.

40 B.-Y. Yu and I.-L. Chien, Design and Optimization of Dimethyl Oxalate (DMO) Hydrogenation Process to Produce Ethylene Glycol (EG), *Chem. Eng. Res. Des.*, 2017, **121**, 173–190, DOI: 10.1016/j.cherd.2017.03.012.

41 G. Giorgianni, C. Mebrahtu, S. Perathoner, G. Centi and S. Abate, Hydrogenation of Dimethyl Oxalate to Ethylene Glycol on Cu/SiO_2 Catalysts Prepared by a Deposition-Decomposition Method: Optimization of the Operating Conditions and Pre-Reduction Procedure, *Catal. Today*, 2022, **390–391**, 343–345, DOI: 10.1016/j.cattod.2021.08.032.

42 J. P. Lange, J. Meurs, M. Rigutto and H. StilA Method of Preparing Glycolic Acid. EP16154238, 2016.

43 J. H. S. Santos, J. T. S. Gomes, M. Benachour, E. B. M. Medeiros, C. A. M. Abreu and N. M. Lima-Filho, Selective Hydrogenation of Oxalic Acid to Glycolic Acid and Ethylene Glycol with a Ruthenium Catalyst, *React. Kinet. Catal. Lett.*, 2020, **131**(1), 139–151, DOI: 10.1007/s11144-020-01843-3.

44 T. K. Slot, P. Oulego, Z. Sofer, Y. Bai, G. Rothenberg and N. R. Shiju, Ruthenium on Alkali-Exfoliated Ti3(Al0.8Sn0.2) C2 MAX Phase Catalyses Reduction of 4-Nitroaniline with Ammonia Borane, *ChemCatChem*, 2021, **13**(15), 3470–3478, DOI: 10.1002/cctc.202100158.

45 C. Hernandez-Mejia, E. S. Gnanakumar, A. Olivos-Suarez, J. Gascon, H. F. Greer, W. Zhou, G. Rothenberg and N. R. Shiju, Ru/TiO 2 -Catalysed Hydrogenation of Xylose: The Role of the Crystal Structure of the Support, *Catal. Sci. Technol.*, 2016, **6**(2), 577–582, DOI: 10.1039/C5CY01005E.

46 S. Akiyama, T. Kakio, S. Indou, R. Oikawa, K. Ugou, R. Hiraki, M. Sano, T. Suzuki and T. Miyake, Preparation of Ru-Sn/C Catalysts and Their Performance in Hydrogenation of Lactic Acid, *J. Jpn. Pet. Inst.*, 2014, **57**(5), 216–224, DOI: 10.1627/jpi.57.216.

47 Y. Takeda, T. Shoji, H. Watanabe, M. Tamura, Y. Nakagawa, K. Okumura and K. Tomishige, Selective Hydrogenation of Lactic Acid to 1,2-Propanediol over Highly Active Ruthenium-Molybdenum Oxide Catalysts, *ChemSusChem*, 2015, **8**(7), 1170–1178, DOI: 10.1002/cssc.201403011.

48 Y. Takeda, Y. Nakagawa and K. Tomishige, Selective Hydrogenation of Higher Saturated Carboxylic Acids to Alcohols Using a ReOx-Pd/SiO_2 Catalyst, *Catal. Sci. Technol.*, 2012, **2**(11), 2221–2223, DOI: 10.1039/c2cy20302b.

49 Y. Takeda, M. Tamura, Y. Nakagawa, K. Okumura and K. Tomishige, From Chip-in-a-Lab to Lab-on-a-Chip: Towards a Single Handheld Electronic System for Multiple Application-Specific Lab-on-a-Chip (ASLOC), *Catal. Sci. Technol.*, 2014, **6**, 5668, DOI: 10.1039/c6cy00335d.

50 J. Pang, M. Zheng, X. Li, Y. Jiang, Y. Zhao, A. Wang, J. Wang, X. Wang and T. Zhang, Selective Conversion of Concentrated Glucose to 1,2-Propylene Glycol and Ethylene Glycol by Using RuSn/AC Catalysts, *Appl. Catal., B*, 2018, **239**, 300–308, DOI: 10.1016/j.apcatb.2018.08.022.

51 M. A. Sánchez, V. A. Mazzieri, S. Pronier, M. A. Vicerich, C. Especel, F. Epron and C. L. Pieck, Ru-Sn-B/TiO 2 Catalysts for Methyl Oleate Selective Hydrogenation. Influence of the Preparation Method and the Chlorine Content, *J. Chem. Technol. Biotechnol.*, 2019, **94**(3), 982–991, DOI: 10.1002/jctb.5849.

52 V. M. Deshpande, K. Ramnarayan and C. S. Narasimhan, Studies on Ruthenium-Tin Boride Catalysts II. Hydrogenation of Fatty Acid Esters to Fatty Alcohols, *J. Catal.*, 1990, **121**(1), 174–182, DOI: 10.1016/0021-9517(90)90227-B.

53 S. M. dos Santos, A. M. Silva, E. Jordão and M. A. Fraga, Performance of RuSn Catalysts Supported on Different Oxides in the Selective Hydrogenation of Dimethyl Adipate, *Catal. Today*, 2005, 107–108, DOI: 10.1016/j.cattod.2005.07.076.

54 A. M. Silva, O. A. A. Santos, M. A. Morales, E. M. Baggio-Saitovitch, E. Jordão and M. A. Fraga, Role of Catalyst Preparation on Determining Selective Sites for Hydrogenation of Dimethyl Adipate over $RuSn/Al_2O_3$, *J. Mol. Catal. A: Chem.*, 2006, **253**(1–2), 62–69, DOI: 10.1016/j.molcata.2006.03.005.

55 A. M. Silva, O. A. A. Santos, M. J. Mendes, E. Jordão and M. A. Fraga, Hydrogenation of Citral over Ruthenium-Tin Catalysts, *Appl. Catal., A*, 2003, **241**(1–2), 155–165, DOI: 10.1016/S0926-860X(02)00463-5.

56 X. Kong, Z. Chen, Y. Wu, R. Wang, J. Chen and L. Ding, Synthesis of Cu–Mg/ZnO Catalysts and Catalysis in Dimethyl Oxalate Hydrogenation to Ethylene Glycol: Enhanced Catalytic Behavior in the Presence of a Mg 2+Dopant, *RSC Adv.*, 2017, **7**(78), 49548–49561, DOI: 10.1039/C7RA09435C.

57 Y. Pouilloux, F. Autin and J. Barrault, Selective Hydrogenation of Methyl Oleate into Unsaturated Alcohols. Relationships between Catalytic Properties and Composition of Cobalt-Tin Catalysts, *Catal. Today*, 2000, **63**(1), 87–100, DOI: 10.1016/S0920-5861(00)00448-X.

58 Y. Pouilloux, F. Autin, C. Guimon and J. Barrault, Hydrogenation of Fatty Esters over Ruthenium–Tin Catalysts; Characterization and Identification of Active Centers, *J. Catal.*, 1998, **176**(1), 215–224, DOI: 10.1006/jcat.1998.2044.

59 X. Kong, Z. Fang, X. Bao, Z. Wang, S. Mao and Y. Wang, Efficient Hydrogenation of Stearic Acid over Carbon Coated Ni Fe Catalyst, *J. Catal.*, 2018, **367**, 139–149, DOI: 10.1016/j.jcat.2018.08.022.

60 T. Toyao, S. M. A. H. Siddiki, A. S. Touchy, W. Onodera, K. Kon, Y. Morita, T. Kamachi, K. Yoshizawa and K. I. Shimizu, TiO2-Supported Re as a General and Chemoselective Heterogeneous Catalyst for Hydrogenation of Carboxylic Acids to Alcohols, *Chem. – Eur. J.*, 2017, **23**(5), 980, DOI: 10.1002/chem.201605679.

61 M. S. Frei, M. Capdevila-Cortada, R. García-Muelas, C. Mondelli, N. López, J. A. Stewart, D. Curulla Ferré and J. Pérez-Ramírez, Mechanism and Microkinetics of Methanol Synthesis via CO2 Hydrogenation on Indium Oxide, *J. Catal.*, 2018, **361**, 313–321, DOI: 10.1016/j.jcat.2018.03.014.

62 Batchington - Catalysis Avantium https://www.catalysis.avantium.com/batchington/(accessed[:] Dec 29, 2021).

63 E. Schuler, P. A. Ermolich, N. R. Shiju and G. -J. M Gruter, Monomers, from CO 2 : Superbases as Catalysts for Formate–to–Oxalate Coupling, *ChemSusChem*, 2021, **14**(6), 1517–1523, DOI: 10.1002/cssc.202002725.

64 E. Schuler, M. Stoop, N. R. Shiju and G.-J. M. Gruter, Stepping Stones in CO 2 Utilization: Optimizing the Formate to Oxalate Coupling Reaction Using Response Surface Modeling, *ACS Sustainable Chem. Eng.*, 2021, **9**(44), 14777–14788, DOI: 10.1021/acssuschemeng.1c04539.

65 B. Wang and G. J. M. Gruter, Polyester Copolymer., WO2018211132A1, 2017.

66 B. Wang and G. J. M. Gruter, Polyester Copolymer., WO2018211133A1, 2017.

67 B. Wang, G. M. Gruter, R.-J. van Putten and D. H. Weinland, Process for the Production of One or More Polyester Copolymers, Method for the Preparation of One or More Oligomers, Oligomer Composition and Polyester Copolymer. WO2020106144A1, 2019.

68 M. Ronda-Lloret, V. S. Marakatti, W. G. Sloof, J. J. Delgado, A. Sepúlveda-Escribano, E. V. Ramos-Fernandez, G. Rothenberg and N. R. Shiju, Butane Dry Reforming Catalyzed by Cobalt Oxide Supported on Ti2AlC MAX Phase, *ChemSusChem*, 2020, **13**(23), 6401–6408, DOI: 10.1002/cssc.202001633.

69 M. Ronda-Lloret, L. Yang, M. Hammerton, V. S. Marakatti, M. Tromp, Z. Sofer, A. Sepúlveda-Escribano, E. V. Ramos-Fernandez, J. J. Delgado, G. Rothenberg, T. Ramirez Reina and N. R. Shiju, Molybdenum Oxide Supported on Ti3AlC2 Is an Active Reverse Water-Gas Shift Catalyst, *ACS Sustainable Chem. Eng.*, 2021, **9**(14), 4957–4966, DOI: 10.1021/acssuschemeng.0c07881.

70 C. Delhomme, D. Weuster-Botz and F. E. Kühn, Succinic Acid from Renewable Resources as a C 4 Building-Block Chemical—a Review of the Catalytic Possibilities in Aqueous Media, *Green Chem.*, 2009, **11**(1), 13–26, DOI: 10.1039/B810684C.

71 Z. Shao, C. Li, X. Di, Z. Xiao and C. Liang, Aqueous-Phase Hydrogenation of Succinic Acid to γ-Butyrolactone and Tetrahydrofuran over Pd/C, Re/C, and Pd–Re/C Catalysts, *Ind. Eng. Chem. Res.*, 2014, **53**(23), 9638–9645, DOI: 10.1021/IE5006405.

72 C. You, C. Zhang, L. Chen and Z. Qi, Highly Dispersed Palladium Nanoclusters Incorporated in Amino-Functionalized Silica Spheres for the Selective Hydrogenation of Succinic Acid to γ-Butyrolactone, *Appl. Organomet. Chem.*, 2015, **29**(10), 653–660, DOI: 10.1002/AOC.3342.

73 K. Yakabi, A. Jones, A. Buchard, A. Roldan and C. Hammond, Chemoselective Lactonization of Renewable Succinic Acid with Heterogeneous Nanoparticle Catalysts, *ACS Sustainable Chem. Eng.*, 2018, **6**(12), 16341–16351, DOI: 10.1021/ACSSUSCHEMENG.8B03346/SUPPL_FILE/SC8B03346_SI_001.PDF.

